Chapter 6

Thermal Stability, Crystallization Kinetics and Morphology of a New Semicrystalline Polyimide based on 1,3-bis (4-aminophenoxy) benzene (TPER) and 3,3’, 4,4’-biphenyltetracarboxylic dianhydride (BPDA).

Abstract

This work investigates the crystallization kinetics and thermal stability of a new melt processable semicrystalline polyimide (Tg= ca. 210°C, T_m= ca. 395°C) based on 1,3-bis(4-aminophenoxy) benzene (TPER) and 3,3’,4,4’-biphenyltetracarboxylic dianhydride (BPDA), and endcapped with phthalic anhydride (PA). Earlier studies have demonstrated that this polymer is a strong candidate as a structural adhesive for high temperature and high performance applications. This study deals with the thermal stability, the effect on crystallization kinetics, and the crystalline morphology of the polymer when exposed to melt temperatures in excess of 410°C for various residence times. In the present study, an Avrami analysis was utilized to study the overall bulk crystallization kinetics after a specific thermal history. The Avrami exponent (n) slightly increased and the parameter ‘K’ decreased with increasing supercooling. Also, Avrami analysis (at 355°C) was utilized to evaluate the effect of melt temperature (from 410°C to 450°C) and effect of melt residence time (2 min to 30 min at 430°C) on the crystallization kinetics. The increase in melt temperature led to an increase in the value of Avrami exponent while the value of parameter ‘K’ dropped significantly. Although the melt residence time did not have much effect on the Avrami exponent, a significant drop in the value of parameter ‘K’ was observed with increasing residence time in the melt. To evaluate the thermal stability, melt viscosity was followed at 430°C as a function of frequency. The melt displayed shear-thinning behavior with a significant drop in viscosity with increasing frequency. Also, the isothermal viscosity at lower frequencies increased by nearly an order of magnitude after ca. 20 minutes at 430°C. Isothermal time sweeps of the melt viscosity were carried out at

different melt temperatures (410°C-450°C) for up to 20 minutes. By increasing the melt temperature, the viscosity increased at faster rates with time, the rate of increase being significantly more above 430°C. Crystallization was investigated by rheological experiments when cooled from the above harsh thermal histories at 10°C/min. With increasing isothermal melt temperature, the onset of crystallization occurred at higher supercoolings. Optical microscopy was utilized to follow the growth rates of the spherulites from the melt at 345°C after quenching from the different melt temperatures. The growth rates decreased significantly as the melt temperature was increased beyond 430°C. Non-isothermal experiments using a DSC were carried out from different melt temperatures. Both optical microscopy and DSC analysis gave evidence of a distinct 'catastrophic nucleation' process at temperatures in vicinity of 330°C.

6.1 Introduction

Aromatic based polyimides are an important subset of high performance and high temperature polymers which, due to their outstanding properties, are finding increasing use in applications such as high temperature adhesives, composites, electronics packaging, fibers, foams and as membranes for gas separation[1,2]. Semicrystallinity in polyimides further improves certain mechanical properties[3], thermal stability[4,5], radiation[6] and chemical resistance[7]. However, of the relatively few semicrystalline polyimides available, most rapidly lose their crystallization ability once taken to the required melt temperature, which is often in excess of 380°C. Melt relative to solution processing of these high performance polymers is thought desirable both from an environmental standpoint (to avoid toxic solvents) and also for ease of processing. Recently, a new polyimide was developed in this laboratory that has displayed excellent characteristics from this standpoint. This polyimide (T_g=ca.210°C, T_m= ca. 395°C) is based on 1,3-bis(4-aminophenoxy) benzene (TPER diamine or 1,3(4)APB) and 3,3',4,4'-biphenyltetracarboxylic dianhydride (BPDA)[4,5,8]. It was also very important to fully endcap the chains with phthalic anhydride (PA) to maximize thermal stability[5]. Earlier

DSC melting studies in this laboratory have demonstrated the excellent thermal stability of this polyimide by showing that very little change in the melting behavior occurred, even after 20 min at 430°C[4,5]. Subsequent studies have also shown the outstanding adhesion properties of this polyimide to titanium alloy, e.g. average lap-shear strengths of 6600-8400psi at ambient temperatures. The adhesive bonds were also stable to a variety of solvents, high temperature aging and elevated test temperatures of 177°C and 232°C[4].

However, for such high temperature thermoplastic polymers processed from the melt, melt time and temperature become important variables from processing and thermal stability viewpoints. Side reactions like crosslinking, branching or chain scission, that may occur at these high melt temperatures usually lead to build up in the molecular weight, and will not only change the rheolgical behavior but may also result in reduced crystallinity and slower crystallization kinetics. On the positive side, the rise in the molecular weight usually leads to improvement of certain mechanical properties, like higher elongation to break and increased toughness. Thus if the rise in molecular weight can be limited to an extent, such that the crystallization kinetics and the amount of crystallinity are not affected much, than a synergistic effect can be produced. In order to obtain this synergism however, it is important to evaluate the rheological behavior at these melt temperatures and the crystallization response when the polyimide is cooled from these harsh melt conditions. The effect of various melt conditions on the subsequent crystallization response also serves as a direct tool in evaluating the thermal stability of the system.

This work examines some of these later issues in detail such as the effect of melt holding conditions on isothermal crystallization kinetics and on the related morphology. Avrami analysis using the DSC and corresponding polarized optical microscopy (POM) experiments were utilized to individually understand the effect of 1) crystallization temperature, 2) melt time and 3) melt temperature on the crystallization kinetics and the resulting morphology of the system.

Melt viscosity studies were conducted at various temperatures to detect the presence of any chemical changes and to ascertain the effect on subsequent crystallization. Non-isothermal studies were also performed using the DSC and hot stage POM to understand the effect of previous melt holding conditions on the subsequent crystallization behavior and semicrystalline morphology of the polyimide.

6.2 Experimental

The details specifying the synthesis of this polymer has been described elsewhere[3,4]. This study, however, will only utilize M_n=15,000 daltons (M_w=30,000 daltons) molecular weight version of this polymer which facilitates a low melt viscosity. However, the molecular weight is sufficiently so as to high to demonstrate good physical behavior (creasable films).

Polarized optical microscopy was performed on a Zeiss optical microscope equipped with a Linkam 600 hot stage, a 35mm camera and a video camera. The hot stage was calibrated using melting point standards and all experiments were conducted under a nitrogen purge. The spherulitic growth rate measurements were performed on thin films (ca. 2 mils) sandwiched between two microscope cover slips. The samples were rapidly heated (ca. 90°C/min) to various melt temperatures and quenched to the desired crystallization temperature (within 15 seconds) using separate nitrogen source. The growth of spherulites was measured as function of time using a Boeckeler Video measurement system. Measurements were performed on 4-6 spherulites in a given sample and the average is reported.

DSC experiments for both isothermal and non-isothermal crystallization were performed on a Perkin Elmer DSC-7. The amount of polymer utilized in a given thermal scan was kept between 6-8 mg. The DSC was calibrated with indium and zinc standards. All experiments were conducted under a nitrogen purge and a DSC baseline was determined by running empty pans. For isothermal crystallization experiments, the samples were kept at room temperature and purged with nitrogen for 5 minutes to remove air from the DSC cell. The samples were then rapidly heated to the desired melt temperatures and kept at that temperature for the desired amount of time. Cooling from these melt temperatures to specific crystallization temperatures was conducted at 200°C/min. In this regard, data collection at high supercoolings was hampered by the initial instability of the DSC signal. This initial instability occurs on cooling to the crystallization temperature at fast cooling rates and may persist for ca. one minute on Perkin Elmer DSC 7 utilized in this study. At higher supercooling, the induction times are short and crystallization is so fast that it is nearly over before the DSC signal has equilibrated. To obtain the initial portion of the exotherm at these temperatures, the straight line from the beginning of the exotherm was extended to the horizontal baseline drawn from the end of the exotherm. The intersection of these two lines was taken as the start of the crystallization exotherm. Such a procedure was attempted for higher degrees of supercooling only when a sufficient straight-line portion of the initial exotherm was available.

Rheological measurements were performed using a Rheometrics RMS-800 rheometer equipped with a 25 mm parallel plate tooling. The experiments were conducted using a percent strain of 5% and the gap between the plates was set at 1.6 mm. All the experiments were carried out in a nitrogen environment. To prepare the specimens, 1.5 grams of the polymer film was compacted at 300°C under a pressure of more than 20 MPa to yield circular discs. These discs were inserted between the circular plates of the rheometer, which were already preheated to 10-15°C above the designated temperature. Although the temperature usually decreased 20-30°C while inserting the samples, the predetermined temperature was again quickly attained by fast heating. The sample was compacted and the polymer that had squeezed out of the ends was scraped off. The data was collected from the time the material again reached the desired temperature and these time sweep experiments were conducted at temperatures of 410, 420, 430, 440 and 450°C for a period of 20 minutes at a frequency of 1 radian/second. To observe the rheology of supercooled melts, all the samples used for time sweep experiments were cooled at a rate of 10°C/ minute while the percent strain and frequency were unchanged. These tests were stopped after crystallization of the sample was observed and the torque had exceeded 500 g.cm. Tests were also conducted to examine the change in complex viscosity when the angular frequency was varied from 0.1 to 100 radians/sec while keeping the strain amplitude constant at 5% and the temperature held at 430°C. Viscosity at the highest frequency was measured first while the lowest frequency was determined last. It took ca. 8 minutes for one such isothermal 'frequency sweep' while four such consecutive sweeps were carried out on the same sample.

6.3 Results and discussion

Although the various experimental[9] and theoretical complications[10,11,12,13] associated with the traditional isothermal Avrami analysis are well recognized, it continues to be the most widely used means of describing the overall bulk isothermal crystallization of polymers. Also, its use together with direct morphological information using microscopy yields important information about the crystallization mechanism and kinetics of a given polymer. In this regard, the Avrami equation is generally written as:

$$X_c(t) = 1\text{-}\exp(-Kt^n) \qquad \{6.1\}$$

In this equation, $X_c(t)$ is the normalized crystalline content at time t. 'K' and 'n' are Avrami constants and are indicative of crystallization mechanisms that are involved. The exponent 'n' in the Avrami equation can provide information on nucleation type and crystal growth geometry. 'K' is dependent upon the shape of the growing crystalline entities (for e.g., whether they are spheres, discs or rods), as well as the type and amount of nucleation (sporadic or predetermined) and the linear growth rate 'G' of the growing crystalline moieties. For example, in case of three-dimensional predetermined spherulitic crystallization 'K' can be expressed as:

$$K=(4\Pi/3)\ N_o\ G^3 \qquad \{6.2\}$$

Here N_o is the nucleation density whereas the exponent of 3 on the growth rate term indicates the Avrami exponent for such a process. The parameters in Eq (1) are usually determined by taking the double logarithm and expressing in the form:

$$\text{Log}\ [-\ln(1-X_c(t))\ ] = \log K + n \log t \qquad \{6.3\}$$

Isothermal DSC analysis is the primary means of performing such an analysis where the normalized crystal fraction $X_c(t)$ is written as :

$$X_c(t)=\Delta H(t)/\Delta H(\infty) \qquad \{6.4\}$$

where $\Delta H(t)$ is the fractional heat of crystallization after time ‘t’ and $\Delta H(\infty)$ being the total heat of crystallization observed at that isothermal crystallization temperature.

An alternate method[14] often used to determine the two Avrami constants utilizes the data for crystallization half time along with Eq (1). However, this method was not used here because of deviations from Avrami behavior at normalized conversions approaching 50%.

Figure 6.1 shows the crystallization exotherms for TPER-BPDA-PA (M_n=15,000 daltons) after quenching from the melt to various crystallization temperatures. As is clearly evident, the overall bulk crystallization is very temperature sensitive in the narrow 20°C range of 340°C to 360°C. Although the rate of crystallization at 360°C is slow as evidenced by a broad crystallization exotherm, an increase in the degree of supercooling by 20°C leads to a large increase in the rate of crystallization. This change in rate of bulk crystallization is reflected in crystallization half-time ($t_{1/2}$), the time to complete 50% of the total crystallization, which decreases from ca. 20 minutes at 360°C to 1.38 minutes at 340°C! At crystallization temperatures higher than 360°C, the crystallization is very slow and the exothermic signal approaches the sensitivity of DSC making collection of reliable data difficult. Collection of isothermal data below 340°C was not possible as the crystallization half time at those temperatures is less than the time it takes for the DSC signal to become stable (ca. one minute). Crystallization of this polyimide (M_n=11,500 daltons) has also been studied by Cheng, Hsiao and Kreuz[15] who suggest a $t_{1/2}$ time of 12 sec at 350°C after cooling at 320°C/min from a less stringent initial melt condition of 420°C for 10 minutes. Although the effects of initial melt history on $t_{1/2}$ are discussed later in this work, it is important to point out that these conclusions by Cheng and coworkers are believed to be inaccurate. While it is not clear how they measured such a short $t_{1/2}$ (the initial instability in the DSC signal itself always lasts for much more than 12 sec), it is also surprising that they indicate three $t_{1/2}$ data points below the glass transition temperature (T_g of 220°C as indicated in their paper).

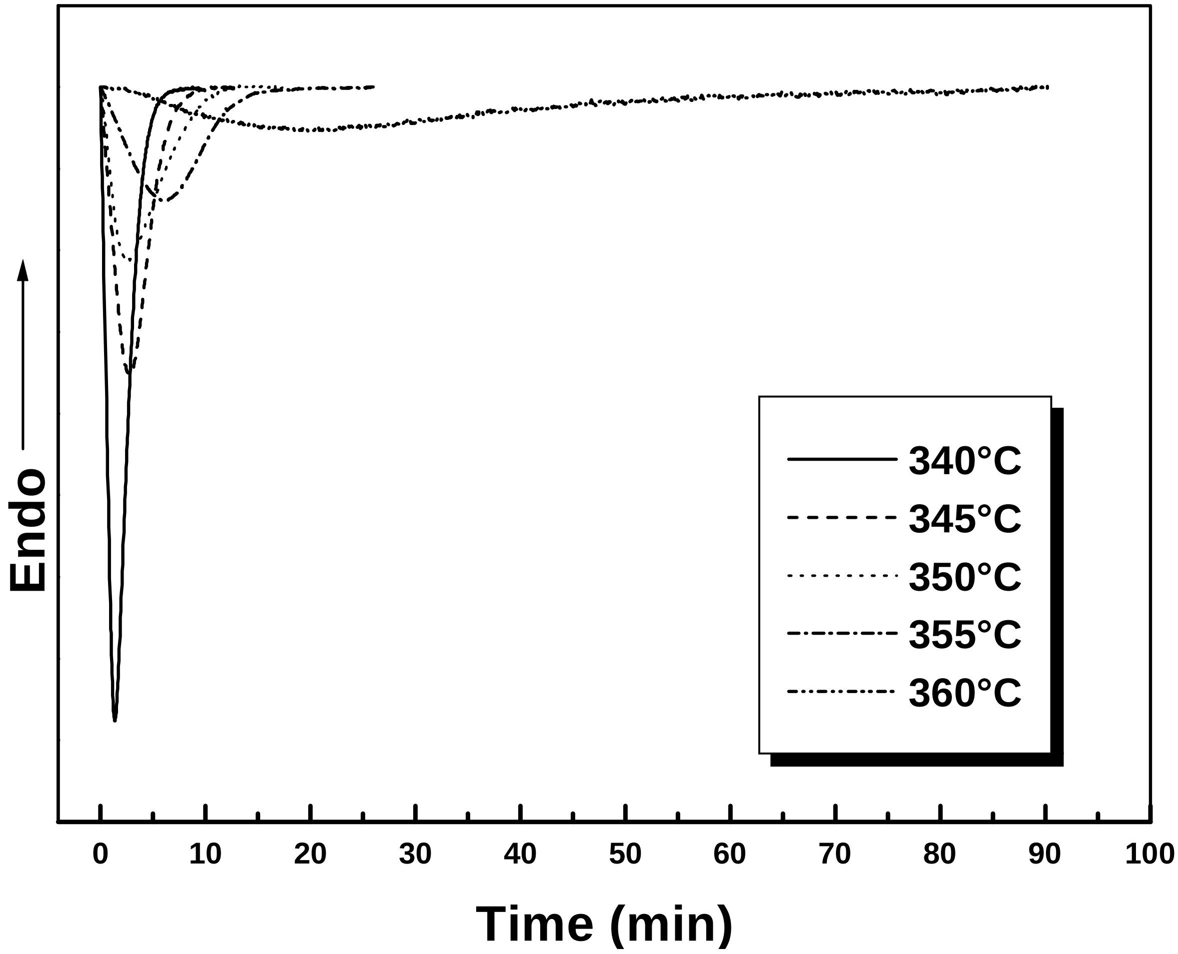

Figure 6.1 Crystallization exotherms at various crystallization temperatures for TPER-BPDA-PA after 20min residence time at 430°C.

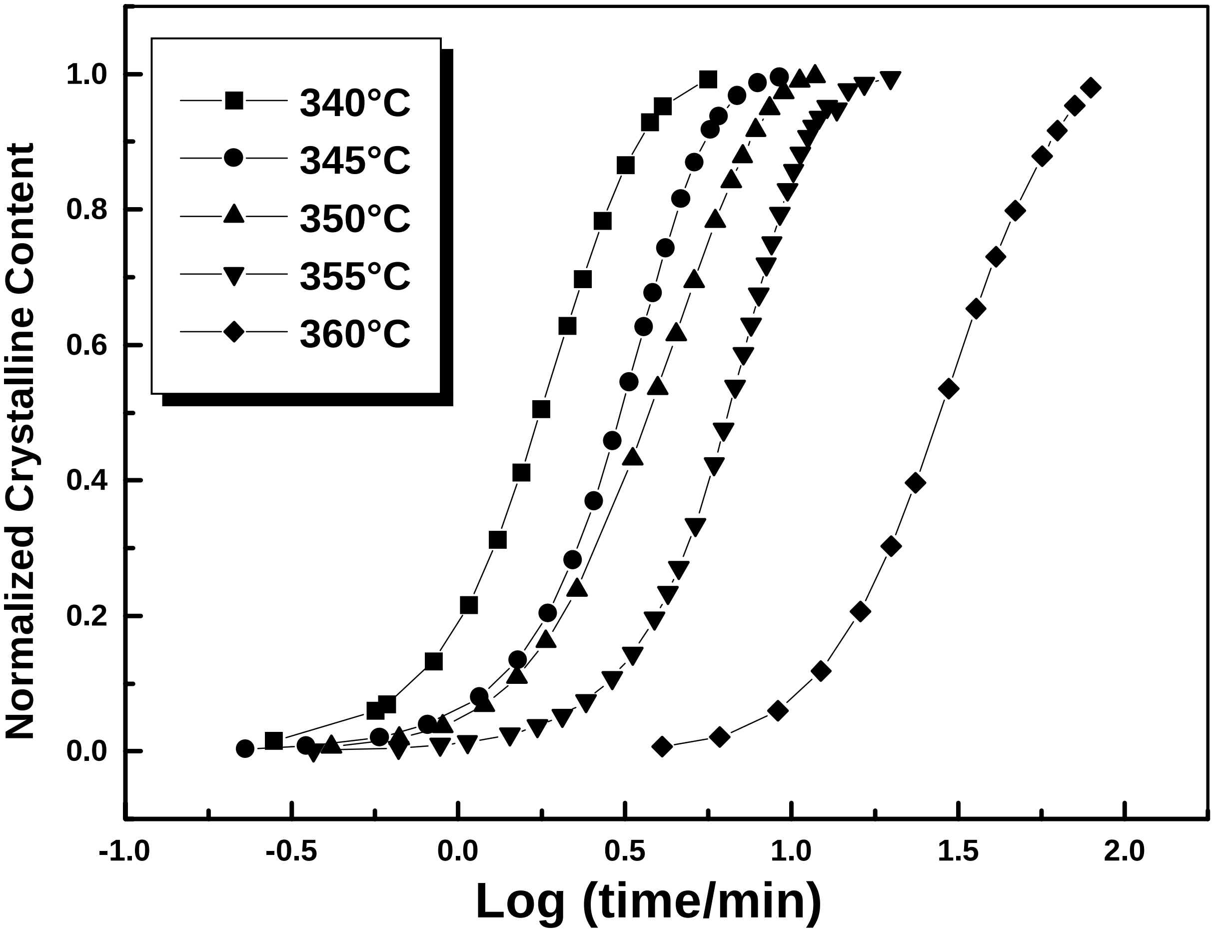

Figure 6.2(a) Normalized crystalline content as a function of Log (time) at various crystallization temperatures.

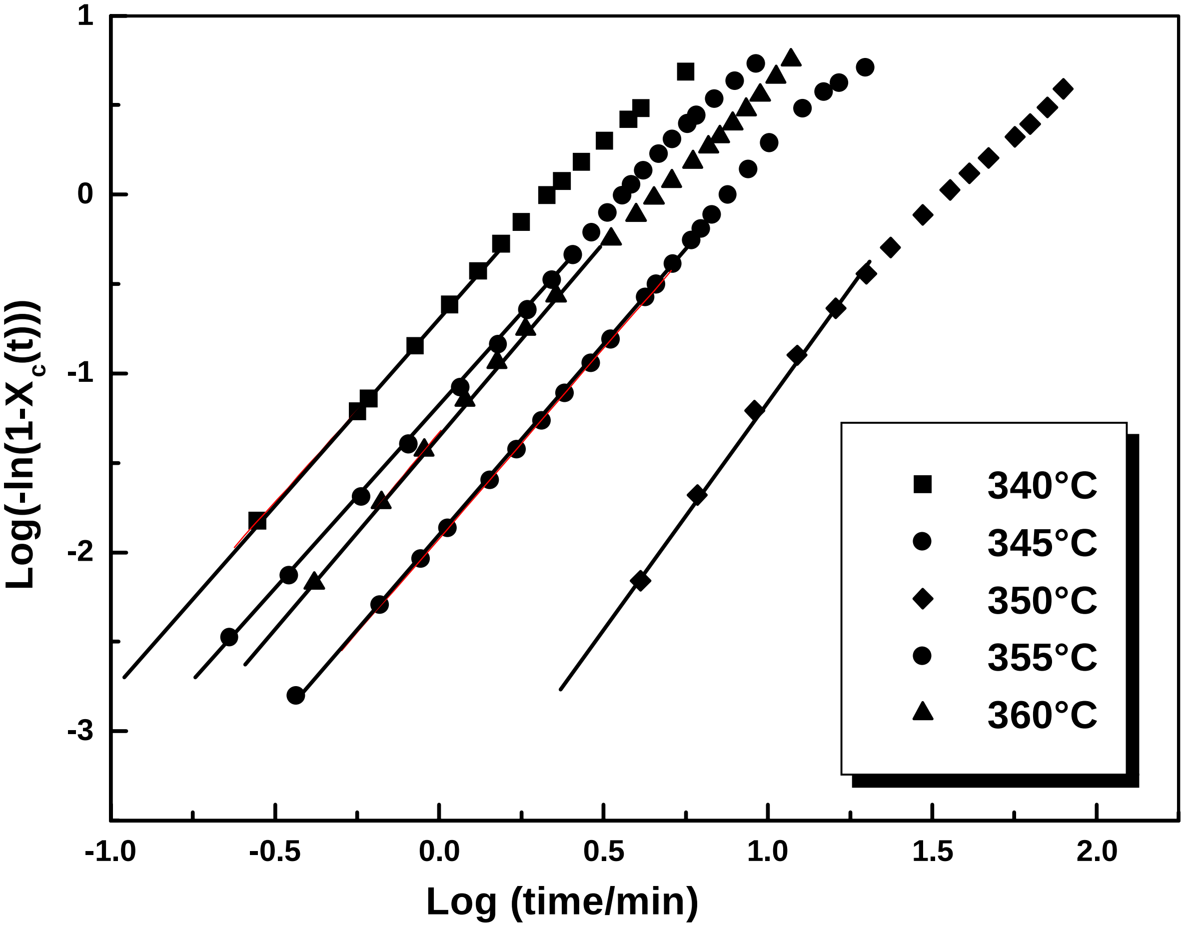

Figure 6.2(b) Plot of log [-ln (1-X_c (t))] versus log (time) at various crystallization temperatures.

Figure 6.2(a) shows the normalized crystalline content as a function of log (time) for the crystallization temperatures examined in this study. It is observed that crystallization shifts to longer times with every 5°C increase in the crystallization temperature. However, this shift to longer times is most noticeable between crystallization temperatures of 355°C and 360°C. Figure 6.2(b) shows the corresponding Avrami plots for the various crystallization temperatures. The curves show an initial linear section but a change in the slope is observed at longer times. The straight lines fit through the initial section of the curves, however, yield the two important Avrami parameters, 'K' and 'n'. The variation of bulk transformation rate 'K' with crystallization temperature is shown in Figure 6.3. The figure also shows the corresponding changes in crystallization half-time '$t_{1/2}$'. A strong correlation between the value of parameter 'K' and crystallization half time is observed as expected. Crystallization half time, which is a measure of the rate of crystallization, decreases with increasing values of 'K'. Figure 6.4 shows the optical micrographs taken at various crystallization temperatures, the initial melt conditions being identical to the DSC experiments described above. While the nucleation density is low at 355°C, it increases sharply with small increases in the degree of supercooling. Thus it is evident that the final spherulitic size decreases greatly with relatively small changes in the crystallization temperature. In fact, no optically resolvable spherulites were observed at and below 330°C due to a catastrophic increase in the nucleation density. This phenomenon will be addressed later in the paper. A small but noticeable change in the Avrami exponent is also observed with varying crystallization temperature. The Avrami exponent is 2.7 at 360°C whereas it decreases to 2.0 at 345°C and 340°C. However, for spherulitic crystallization and a somewhat mixed mode of nucleation observed, the value of the Avrami exponent is expected to be slightly above 3. Although optical microscopy clearly reveals a spherulitic morphology at the discussed crystallization temperatures, the initial growth of such a spherulitic structure may not be truly three-dimensional. Figure 6.5 shows the schematic development of a fully-grown spherulite from an initial single lamella. The presence of an intermediate sheaf like structures would tend to decrease the Avrami exponent from 3 as has also been suggested previously[16, 17]. Also, the Avrami exponent is calculated using the earlier stages of crystallization where the presence of such

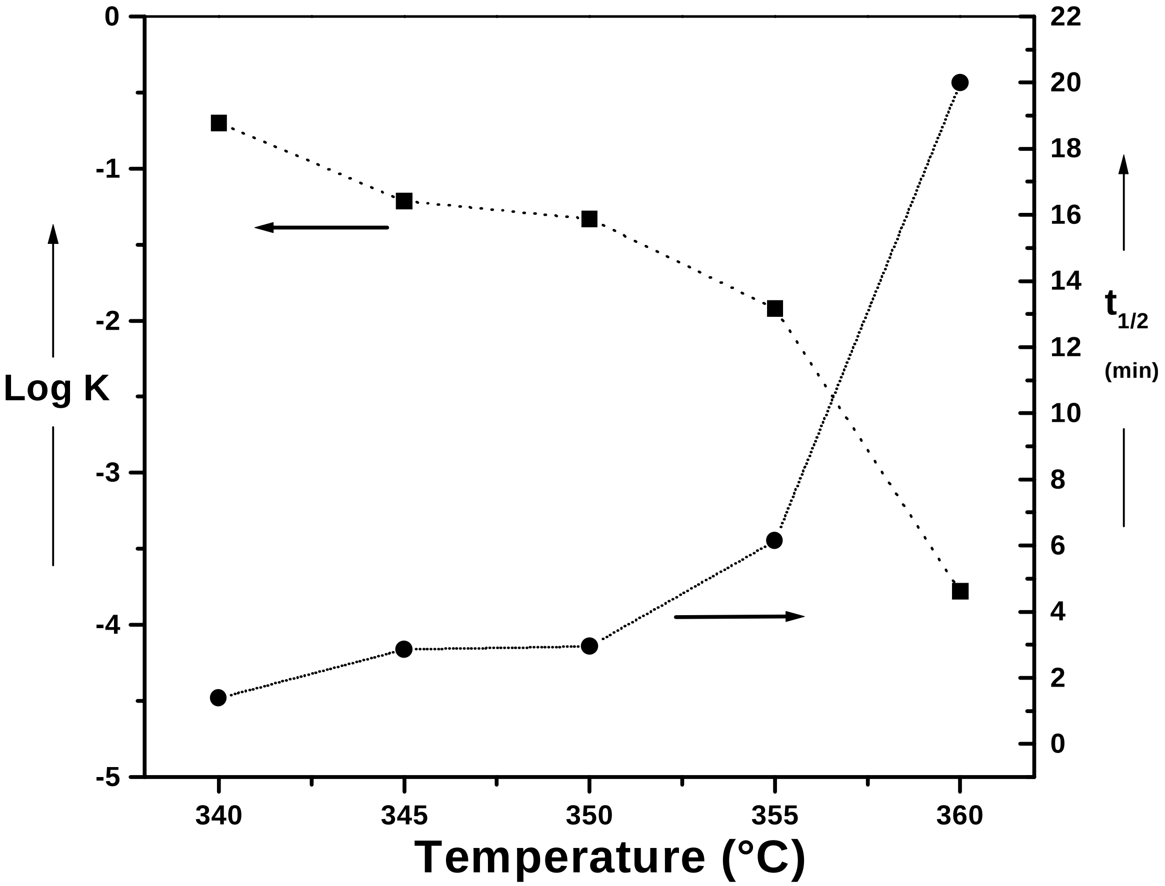

Figure 6.3 Variation of logarithm of transformation rate ‘K’, and crystallization half time ‘$t_{1/2}$’, as a function of crystallization time after melt holding conditions of 430°C for 20 minutes.

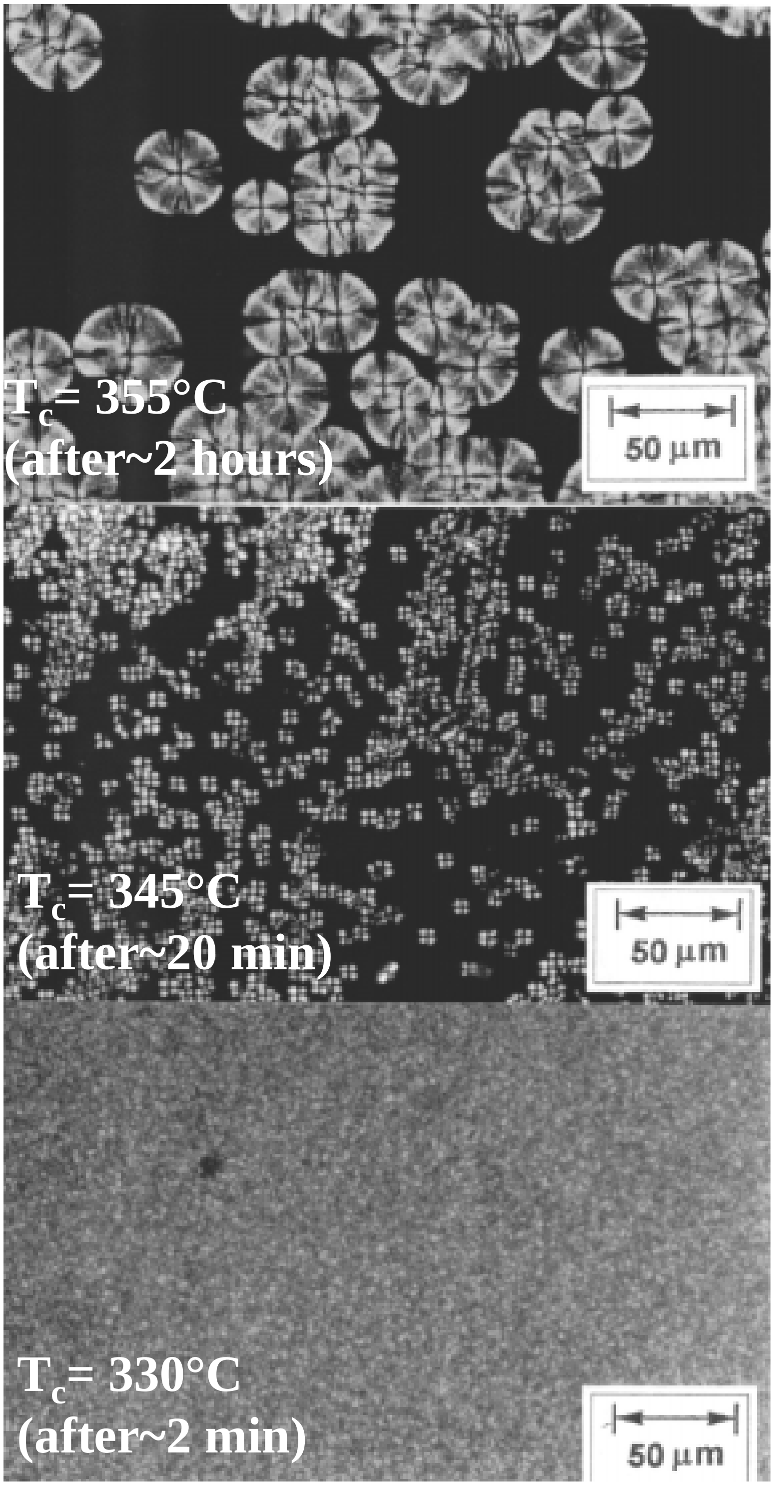

Figure 6.4 Polarized optical micrographs at the indicated crystallization temperatures after being at a melt temperature of 430°C for 20 minutes.

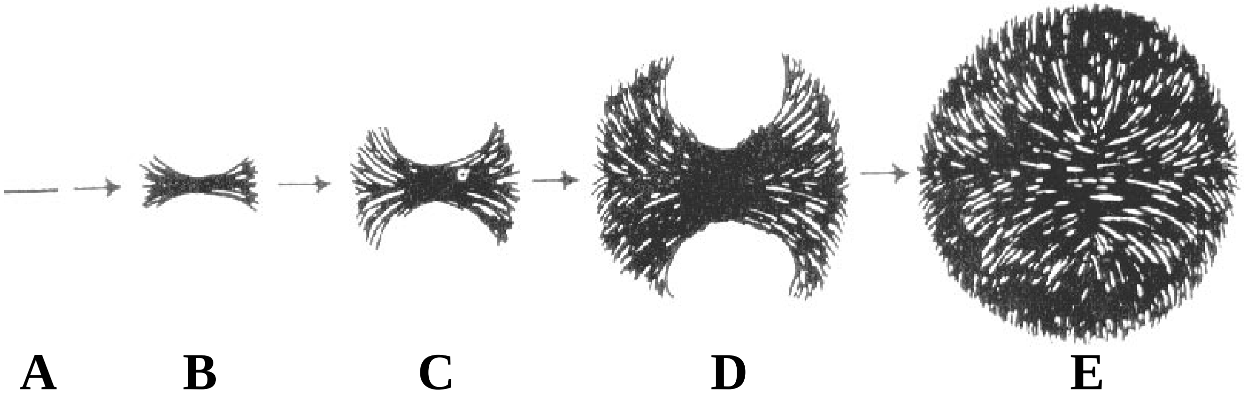

Figure 6.5 Evolution of spherulitic growth ranging from a folded-chain single crystal to a fully developed spherulite[21].

intermediate structures is more likely and thus would contribute to a decreased Avrami exponent. Such an effect may become even more important as the crystallization temperature is lowered and the nucleation density increases. This increase in nucleation density could result in a large number of only partially developed spherulites colliding with each other at an early stage thus giving rise to sheaf-like structures and/or truncated spherulites. This type of geometry would again lower the Avrami exponent.

It is of interest to compare the bulk crystallization rate ‘K’ obtained for this polyimide with similar results obtained for other high performance polymers. However, before making any such comparison it is important to recognize that the units of K depend on the value of the Avrami exponent ‘n’. Thus, in order to make such comparisons, it is more useful to compare the values of $K^{1/n}$. Secondly, the supercooling at which these comparisons are made need to be similar. Also, the initial melt conditions can substantially affect the crystallization rate at a given undercooling. The initial melt temperature, if below the equilibrium melting point, can often result in self-seeding nucleation and thus lead to a higher value of the transformation rate ‘K’. Thus in order to assess the differences in crystallization kinetics and make valid comparisons, it is essential that the initial melt temperatures for the two polymers are above their respective equilibrium melting points. In this regard, Lee and Porter[17] obtained a value of 0.17min^{-1} for $K^{1/n}$ in the case of PEEK at a supercooling of 80°C when cooled from a melt temperature of 370°C (T_m^o=395°C). However the value of $K^{1/n}$ dropped to 0.06min^{-1} at the same undercooling when the melt temperature was increased to 410°C (due to possible crosslinking at that temperature). Cebe and Hong[18] noted a value of 0.05min^{-1} for PEEK at the ΔT_c of 80°C and 0.22min^{-1} at ΔT_c of 87°C when cooling from 400°C. Cheng[19] et al. obtained a value of 0.01min^{-1} at a ΔT_c of 96°C for a polyimide with flexible ethylene glycol sequence (inherent viscosity 0.68 dL/g) when cooled from above the equilibrium melting point of that polymer. Hsiao[20] et al. obtained a value of 0.04 min^{-1} at a supercooling of 121°C for a commercial semicrystalline polyimide, New-TPI, when cooled from melt at 410°C (T_m^o=406°C). Lopez and Wilkes[21] achieved a value of ca. of 0.71min^{-1} for poly (p-phenylene sulfide) at a ΔT_c of 70°C when cooled from 320°C (T_m^o=312°C). For the semicrystalline polyimide used in this study, the author has obtained a value of 0.45min^{-1}

for $K^{1/n}$ at ΔT_c of ca. 70°C (based on T_m^o of 410°C). However, it is important to state here that this value was obtained after residence times of 20 minutes at 430°C. Smaller residence times at the same temperature would result in even higher value of ‘K’ as will be discussed later. These results thus clearly illustrate the very fast crystallization kinetics demonstrated by this polymer. The bulk crystallization rate ‘K’ depends upon the nucleation mode, nucleation density and the growth rate of the individual crystalline moieties[22]. In this regard, the overall crystallization therefore depends on two factors: (1) the growth rates of the individual spherulites and (2) the number of such spherulites growing (nucleation density).

Figure 6.6 shows the spherulitic growth rates at the various crystallization temperatures discussed earlier. Also, the melt temperature and time of 430°C and 20 minutes used for this study were the same as the melt conditions utilized for the bulk crystallization DSC studies. At a particular crystallization temperature, the radial growth rates were constant with time. The increased growth rates at larger supercooling contribute to a faster crystallization response and this would be reflected in the higher values of ‘K’ obtained at 345°C. The second important contribution to the increase in crystallization rate with increasing supercooling is due to the increase in nucleation density. While the nucleation mode is primarily athermal at 360°C, new spherulites also appear with time at lower crystallization temperatures, indicating some degree of thermal nucleation. This mixed mode of nucleation does not allow for a convenient calculation of a numerical value of the nucleation density using a simple expression like Eq (2) from classical Avrami theory. The contribution of nucleation density to overall crystallization kinetics, however, is clearly revealed by optical microscopy. This large increase in nucleation density obviously greatly increases the overall bulk crystallization rate ‘K’.

Although both faster growth rates and increase in nucleation density contribute to a large increase in the bulk transformation rate, it is important to visualize which of these two factors is more responsible in determining the observed crystallization response. Nucleation mode and value of the Avrami exponent ‘n’ decide the exact form of relationship between the growth rate ‘G’ and the parameter ‘K’ (the growth rate is raised to power n). In this regard, it is meaningful to recognize that although the optical

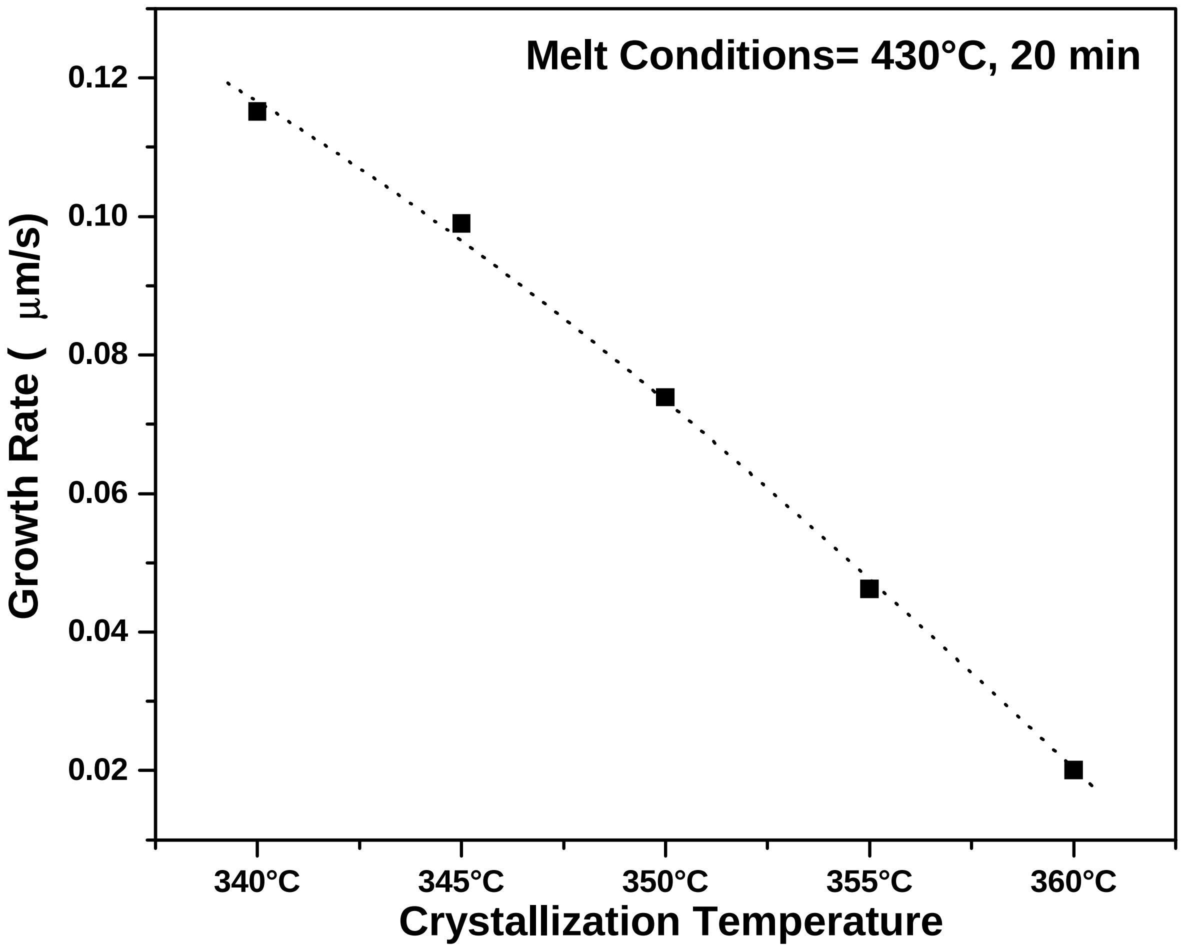

Figure 6.6 Radial growth rates of spherulites at various crystallization temperatures after melt temperature of 430°C for 20 minutes. (M_n=15,000 daltons, M_w=30,000 daltons)

micrographs shown here suggest increasing nucleation density to be more important, small changes in growth rate alone may significantly affect the bulk transformation rate. However, if effects due to nucleation density were absent, than the transformation rate $K^{1/n}$ would scale proportionally with changes in growth rate ‘G’. An estimate of the two competing processes can thus be obtained by comparing the relative changes in ‘$K^{1/n}$’ and ‘G’ at two typical crystallization temperatures of 340°C and 345°C (the value of the Avrami exponent ‘n’ is ca. 2 in both cases). While it is found that the value of $K^{1/n}$ is ca. 82% more at 340°C than at 345°C, the growth rate of the spherulites ‘G’ is only increased by 14% at 340°C. This clearly suggests a strong contribution of nucleation density to increasing the bulk transformation rate. This deduction is also in accordance with the trend observed in the optical micrographs (Figure 6.4).

It is often observed that the overall crystallization consists of two separate parts: the initial stages being indicative of a primary crystallization process while, at later times, a change to a lower slope is often ascribed to secondary crystallization. Secondary crystallization further tends to lower the Avrami exponent by one or more. In this case, these changes in slope of the Avrami curve are prominently observed for higher crystallization temperatures while for lower crystallization temperatures the change in slope is less prominent. Also, this change in slope occurs after ca. 60-70% of the total crystallization. The change in slope at these conversions is also the reason for not using the crystallization half-time method to calculate the two Avrami constants. Also in this case, the deviations in the slope always occur after the peak of the crystallization exotherm. It is often assumed that the likelihood of spherulitic impingement in the bulk of the sample increases in the vicinity of the peak of the crystallization exotherm. Thus it is very likely that the most spherulitic impingement’s take place at times where these changes in slope are observed. These spherulitic impingement’s would further tend to lower the slope. Additionally, the process of secondary crystallization (which also lowers the slope) is expected to be more pronounced once these spherulitic impingement’s have taken place (and the primary crystallization largely stopped). The effects of secondary crystallization on the overall bulk crystallization kinetics have also been observed for numerous other

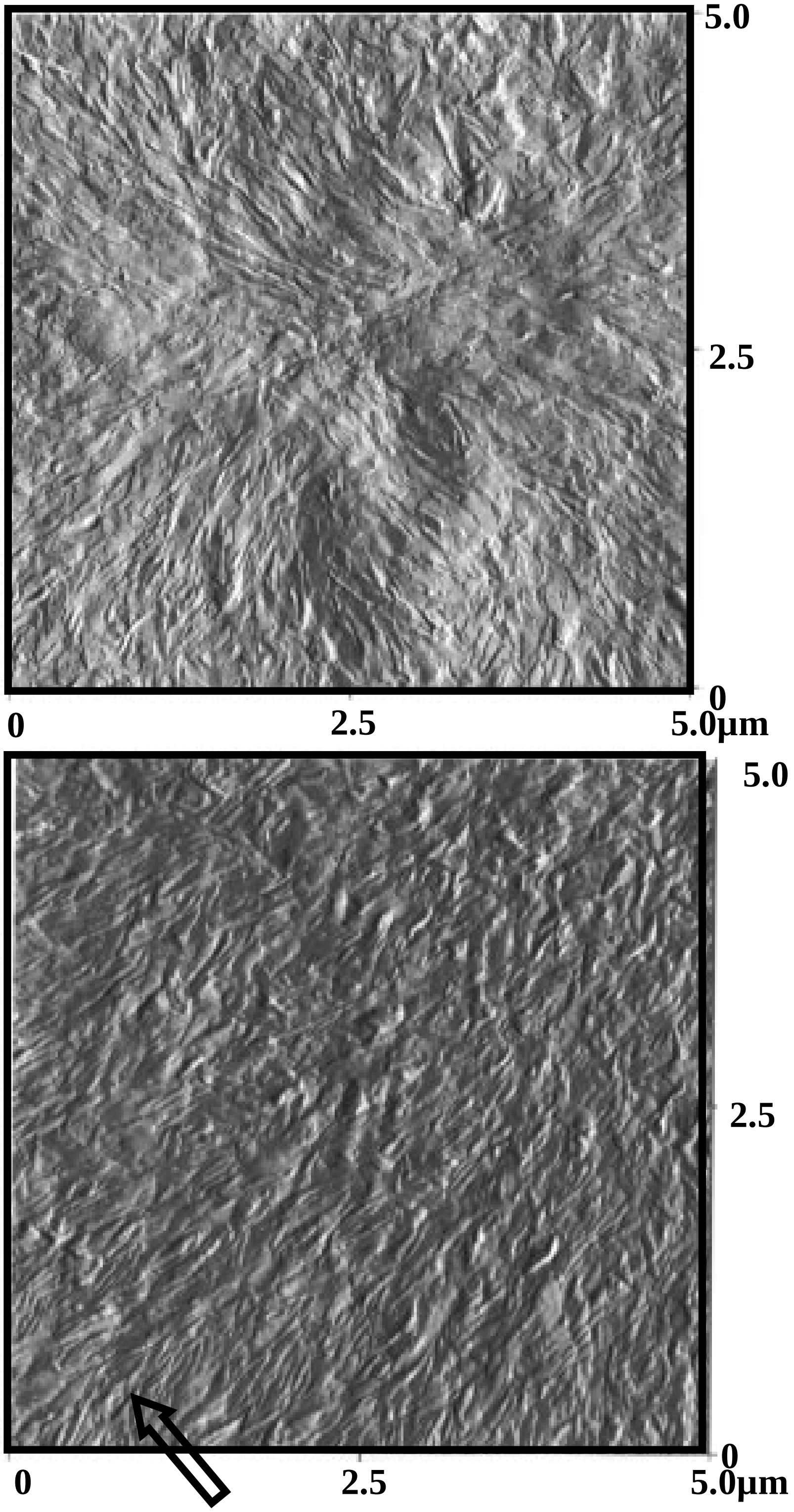

Note Twisting lamellae

Figure 6.7 (a) AFM height image of a central part of a spherulite for a sample crystallized at 360°C after a melt temperature of 430°C for 20 minutes. **(b)** AFM height image of a outward region of a spherulite for a sample crystallized at 360°C after a melt temperature of 430°C for 20 minutes. The center of the spherulite lies toward the upper-right of the micrograph.

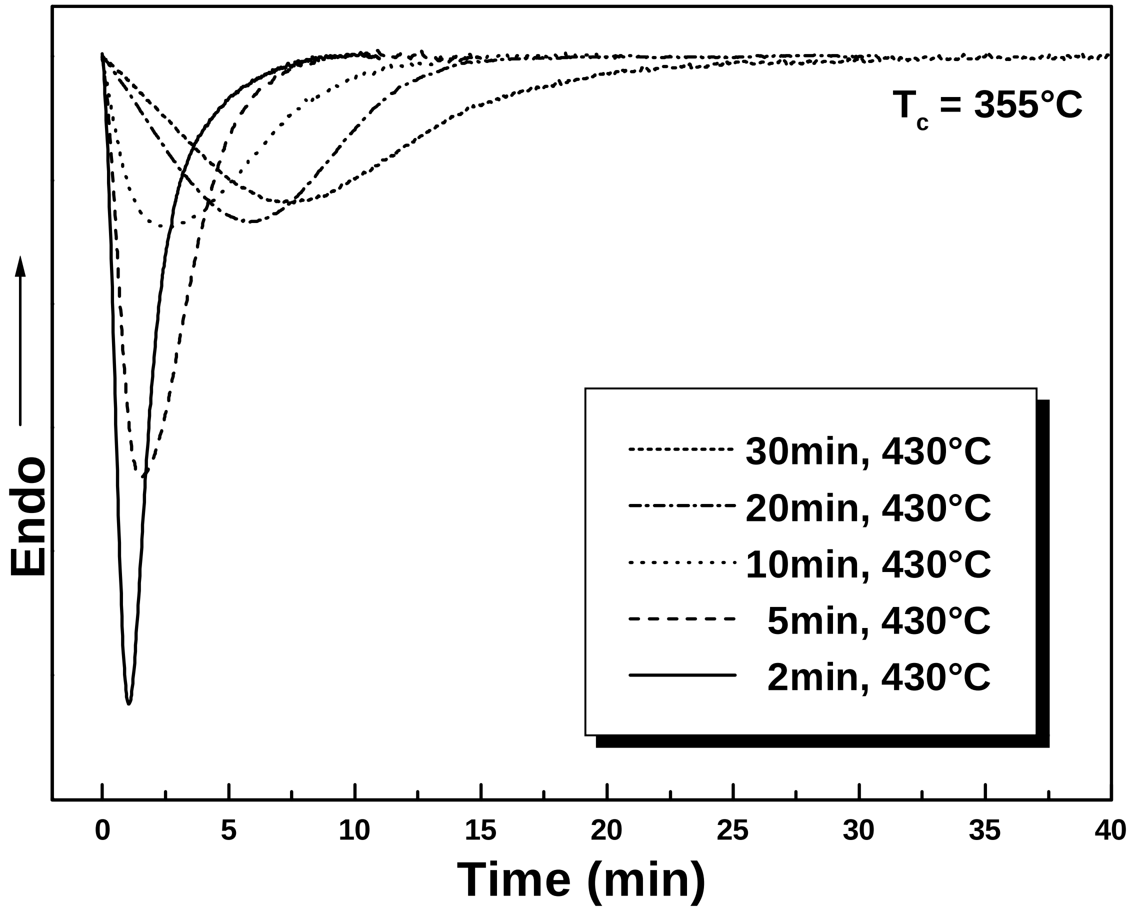

Figure 6.8 Crystallization exotherms at 355°C after various melt residence times at 430°C.

polymers[23] including polyethylene[24,25], PEEK[11, 12,26] and other semicrystalline polyimides[13, 14].

Although, the bulk morphology as revealed by optical microscopy is spherulitic, the underlying lamellar substructure responsible for such final spherulitic development is distinctly discernible by atomic force microscopy. Figure 6.7(a) shows the AFM micrograph of a sheaf like structure present at initial stages of development of a spherulite. Considerable branching of the lamellae in regions away from the center is observed which is finally responsible for a three-dimensional spherulitic structure. Figure 6.7(b) shows the AFM micrograph of a region away from the center of a fully developed spherulite. Outwardly radiating lamellae from the center of the spherulite (the center of the spherulite is towards the bottom-right of the micrograph) are clearly revealed. It is particularly interesting that the fundamental crystalline structure of this polymer is lamellar although the polymer has a rather large repeat unit size (M_u=536 daltons). Also, earlier SAXS studies[3] in this laboratory have yielded average Bragg spacing of ca. 163 Å for this polymer. Considerable twisting of the lamellae ("banding") could also be observed, some of which is visible in Figure 6.7 (b). For POM experiments, banding was observed for the higher crystallization temperatures of 360°C or more (not shown here).

6.3.1 Effect of melt residence time and melt temperature on crystallization kinetics:

Nucleation of macromolecular melts when cooled is critically dependent upon the previous melt temperature and time in the melt. Generally, it is found that the supercooling required to achieve crystallization in a given time, over a certain temperature range, depends strongly on the superheating above the bulk melting temperature of the material. This trend continues till a given degree of heating above the melting temperature after which the crystallization behavior is independent of the melt temperature[16]. Such a behavior is explicable on the basis of thermal history sensitive nucleation proposed by

Turnbull[27]. According to this, the crystalline material present in the crevices and cracks of heterogeneity may wet the surface and thus may require a temperature above the melting point of the material to destroy these sites. *In fact, depending upon the size and the shape of the cracks, and the interfacial surface energy, the dissolution temperature for these sites may considerably exceed the bulk melting temperature*[16, 19, 28]. These sites if not destroyed can serve as possible nucleation sites (heterogeneous nucleation due to residual nuclei) on subsequent cooling. The second type of nucleation that may affect the crystallization behavior is the self-seeding nucleation by crystals surviving the nominal melting point of the polymer[16]. To completely erase the effect due to this type of nucleation, it is often necessary to raise the temperature above the equilibrium melting temperature. The resulting nucleation density on cooling can thus be significantly dependent on the previous melt temperature and position of melt temperature vis a vis the true equilibrium melting point of the polymer. Time in the melt is another important factor that might influence the subsequent crystallization. If exposed for very short amounts of time above the melting temperature, the crystals often reappear at exactly the same place (memory effect)[29]. Also, when the melt temperatures are in excess of 400°C, it becomes important to evaluate the effect of possible degradation reactions on the crystallization kinetics. Chemical changes leading to crosslinking, molecular weight increase, or chain branching may severely inhibit the ability of the system to crystallize. The effect of such severe melt conditions on the crystallization kinetics thus serves as a direct tool in evaluating the thermal stability of the polymer.

Thus Avrami analysis was utilized to examine the effect of melt residence time on isothermal crystallization kinetics at a given crystallization temperature and for a typical melt temperature of 430°C. This melt temperature is in the vicinity of possible melt processing temperatures that this polyimide may experience and was in fact found to be the optimum processing temperature for attaining the best adhesive strengths in an earlier work on the same material[4]. The melt residence times selected were varied between 2 to 30 minutes and are representative of the processing times that may be required for different applications. Figure 6.8 illustrates the crystallization exotherms obtained after cooling to 355°C, the polymer being in the melt at 430°C for the melt residence times

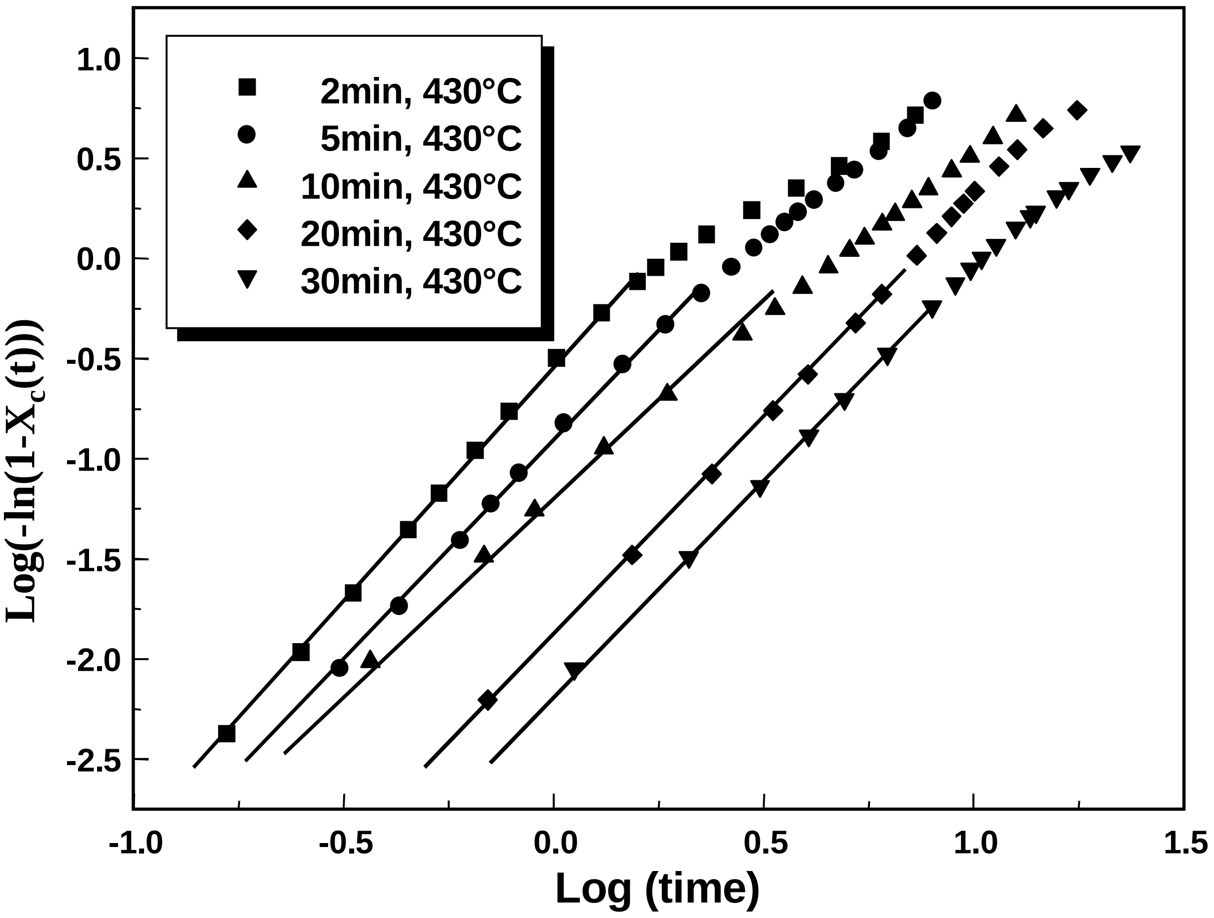

Figure 6.9 Plot of log [-ln (1-X_c (t))] versus log (time) at 355°C after various melt residence times at 430°C.

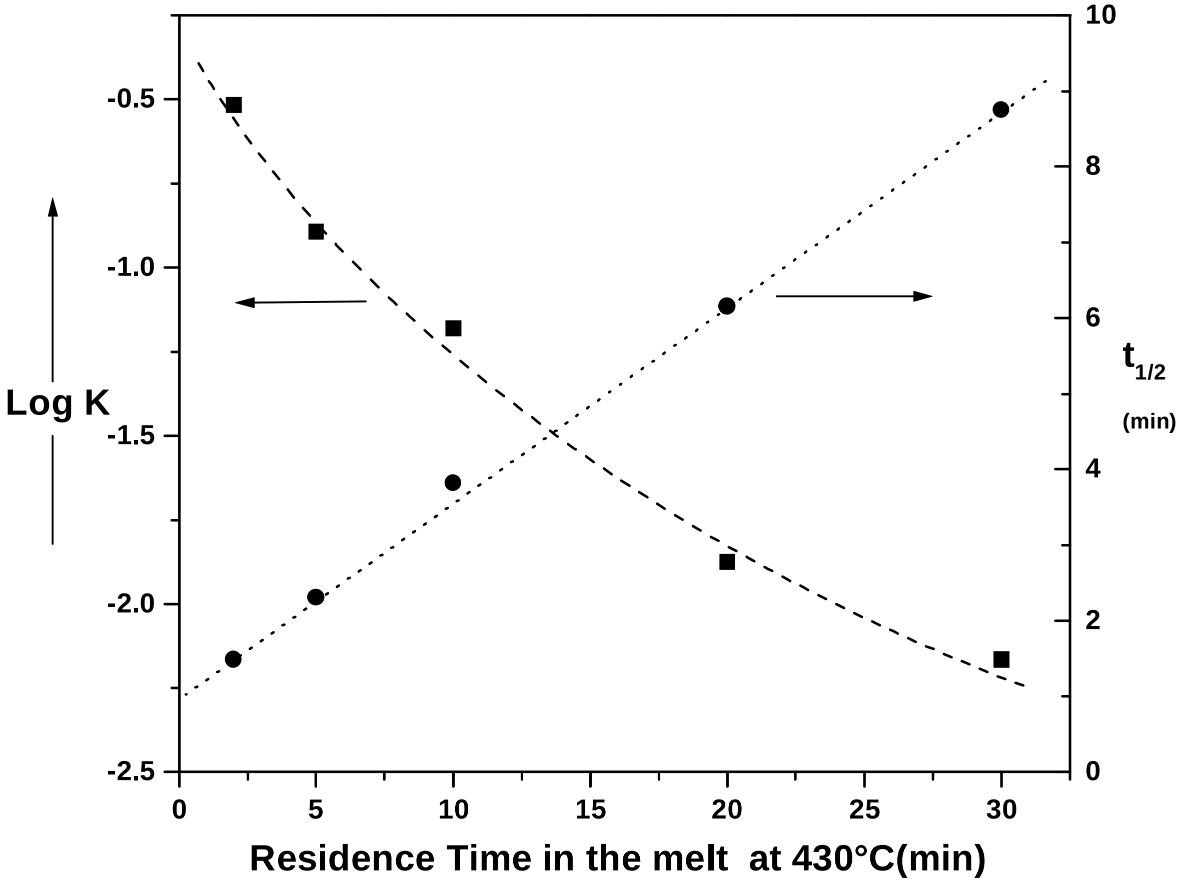

Figure 6.10 Variation of logarithm of transformation rate 'K', and crystallization half time '$t_{1/2}$' at the crystallization temperature of 355°C, as a function of residence time at 430°C.

shown. It is clear that melt residence time has a major effect on the crystallization behavior of TPER-BPDA-PA. Short residence times of only 2 or 5 min result in a relatively faster crystallization response, while an increase in the melt residence times to 10 or 20 min leads to significant slowing down of the crystallization kinetics. For longer residence time of 30 min, the decrease in crystallization rate is also accompanied by significant broadening of the crystallization exotherm. Figure 6.9 shows the corresponding Avrami plot for the exotherms shown in Figure 6.8. It is clear that the crystallization behavior shifts continuously to longer times with increasing residence times in the melt. However, the value of the Avrami exponent did not show much change (n=2.1-2.4) with change in melt residence time. Figure 6.10 depicts the change in the value of the bulk crystallization rate 'K' and the crystallization half-time ($t_{1/2}$) as the residence time in the melt was increased at 430°C. The value of 'K' decreased progressively with increasing residence times in the melt, while $t_{1/2}$ showed a corresponding increase indicating again a slower rate of crystallization. The lower crystallization rate with increasing melt residence times can be due to the slower spherulitic growth and/or lower nucleation density. To examine this aspect, independent optical microscopy measurements were also conducted at the same crystallization temperature and the micrographs are shown in Figure 6.11. The optical micrographs reveal a significant drop in nucleation density with increased residence times in the melt at 430°C. For short residence times, the melt has not become truly homogenous and previous thermal history affects the subsequent crystallization. It is clear that a number of residual nuclei survive these short melt exposure times and serve as nucleation sites on cooling. However, with increasing melt exposure times, the melt becomes more homogenous and reduction in the number of surviving nuclei takes place. This leads to a lower nucleation density as revealed by optical microscopy. Any chemical changes occurring in the melt would also tend to slow down the rates of crystallization if these reactions lead to increases in the molecular weight through chain extension, branching and cross-linking. Later results presented in this paper show evidence of noticeable chemical changes occurring at and above 430°C for longer melt residence times (20min). The cross-linking and branching reactions influence the crystallization kinetics and the amount

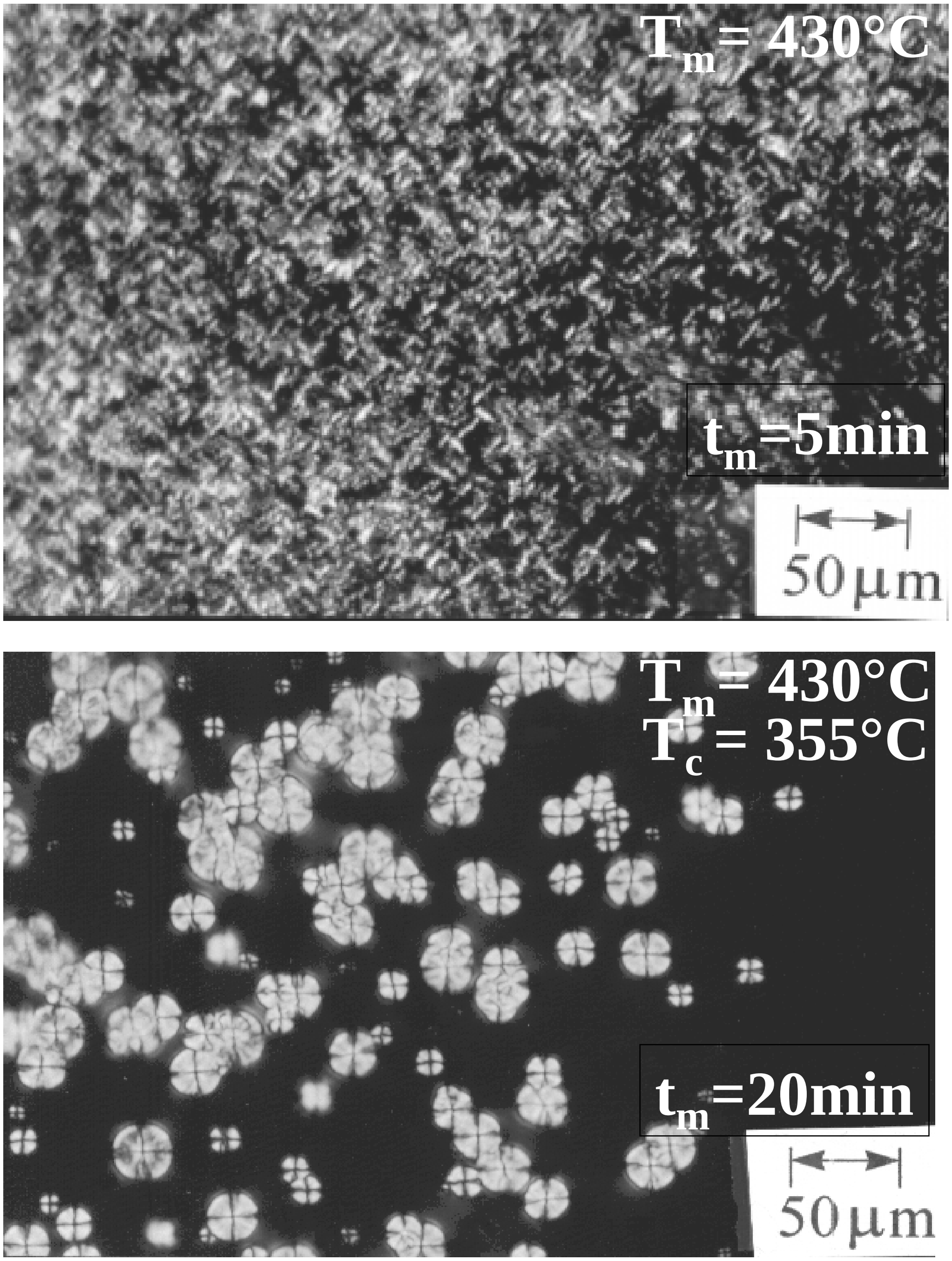

Figure 6.11 Polarized optical micrographs at 355°C after the indicated melt residence times at 430°C.

of these chemical reactions increases with longer melt residence times. The molecular weight increase due to these reactions would also decrease the spherulitic growth rate. However, for the shorter residence times of 2min and 5min, the degradation processes are minimal and thus spherulitic growth rates are not expected to vary much. Yet there is a large difference in the crystallization kinetics as evidenced by the respective crystallization exotherms and values of $K^{1/n}$ obtained from Avrami analysis. While the value of $K^{1/n}$ is $0.61 min^{-1}$ after a residence time of 2min, it decreases to $0.40 min^{-1}$ by increasing the residence time to 5 minutes. This difference is due to decreasing the nucleation density with higher '5 min' residence time. For still higher melt residence times, the degradation reactions which occur result in decreasing the spherulitic growth rates (shown later), which also contribute in slower crystallization kinetics. Thus, while $K^{1/n}$ decreases from $0.40 min^{-1}$ to $0.13 min^{-1}$ as the residence time is increased from 5min to 20min (i.e. by a factor of more than 3), growth rates also decrease by a factor of 2. Therefore, although variations in nucleation density are influencing the crystallization kinetics at shorter residence times, reduced spherulitic growth rates at longer residence times also contribute to decreasing the transformation rates.

Similar effects of the melt residence times on the crystallization behavior would generally be expected for other melt temperatures. Temperatures greater than 430°C lead to a decrease in the isothermal crystallization kinetics while this effect becomes markedly less pronounced for lower melt temperatures. In fact for a melt residence temperature of 410°C, which is close to the bulk melting point, considerable residual nuclei survive much longer residence times, the residual nuclei resulting in an increased rate of crystallization.

Next the influence of melt temperatures on the crystallization kinetics is examined while keeping the melt residence time and the isothermal crystallization temperature constant. Figure 6.12 shows the crystallization exotherms at 355°C after cooling from melt temperatures ranging from 410°C to 430°C for 20 minutes. As can be noted, the melt temperature strongly affects the isothermal crystallization behavior. As the melt temperature is increased, the peak of the crystallization exotherm shifts to longer times. While no considerable broadening is observed, the shapes of the crystallization exotherms change with increasing melt temperatures. As the initial melt temperature is varied from

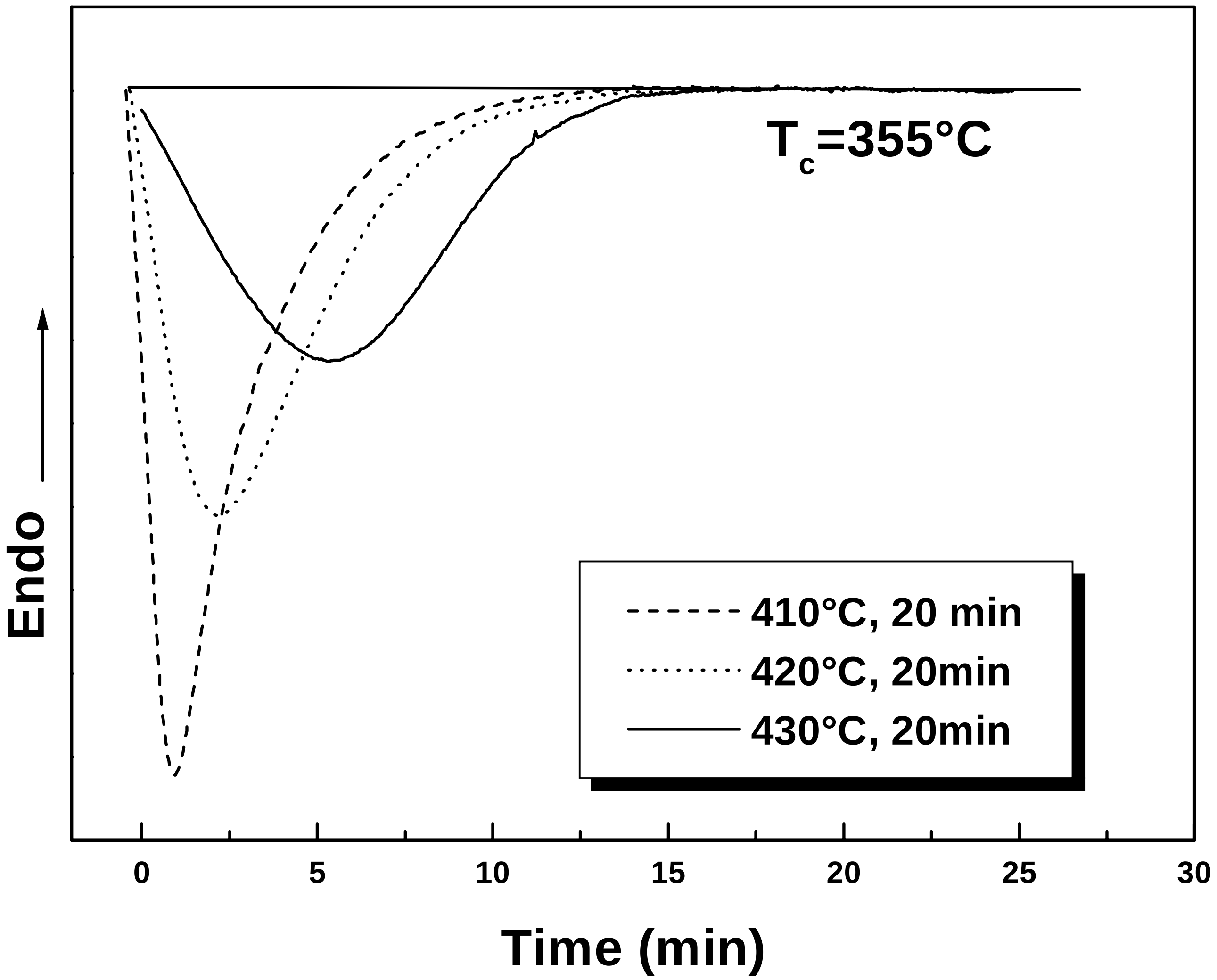

Figure 6.12 Crystallization exotherms at 355°C after a 20 minutes residence time at various melt temperatures.

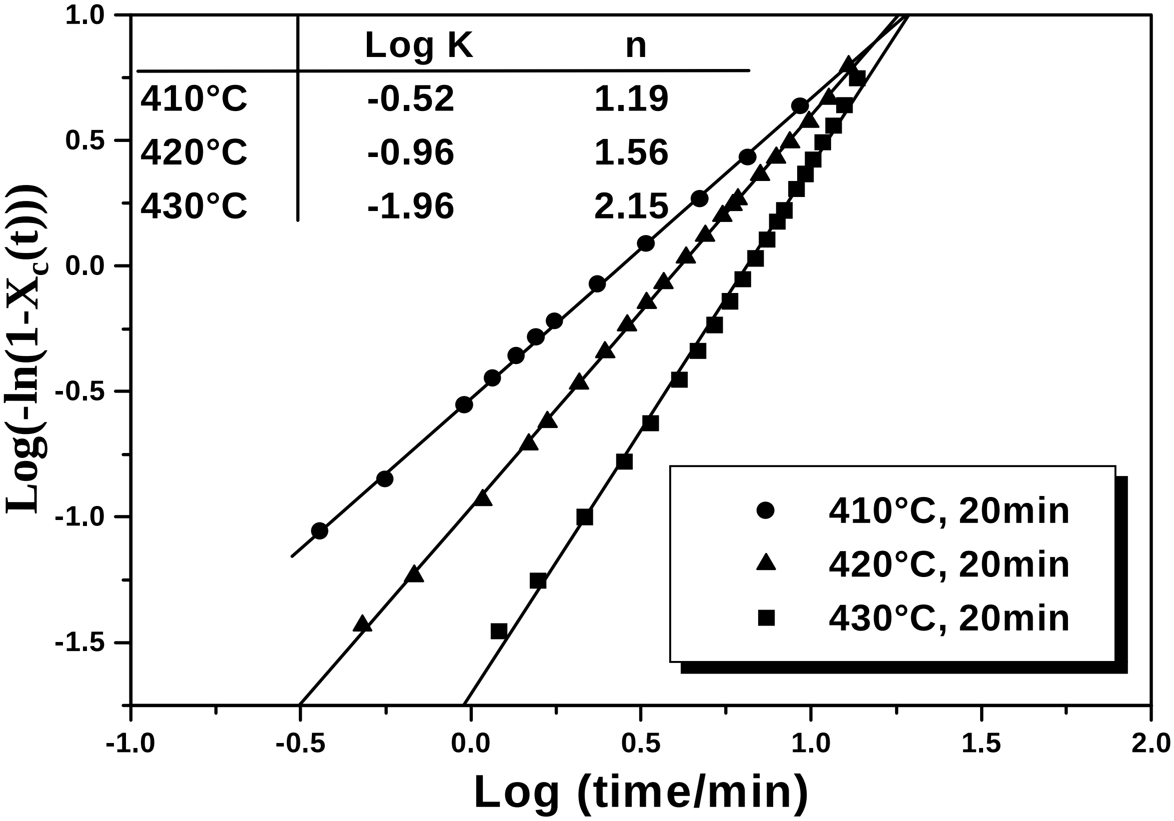

Figure 6.13 Plot of log [-ln (1-X_c (t))] versus log (time) at 355°C after various melt temperatures and a 20 minutes residence time.

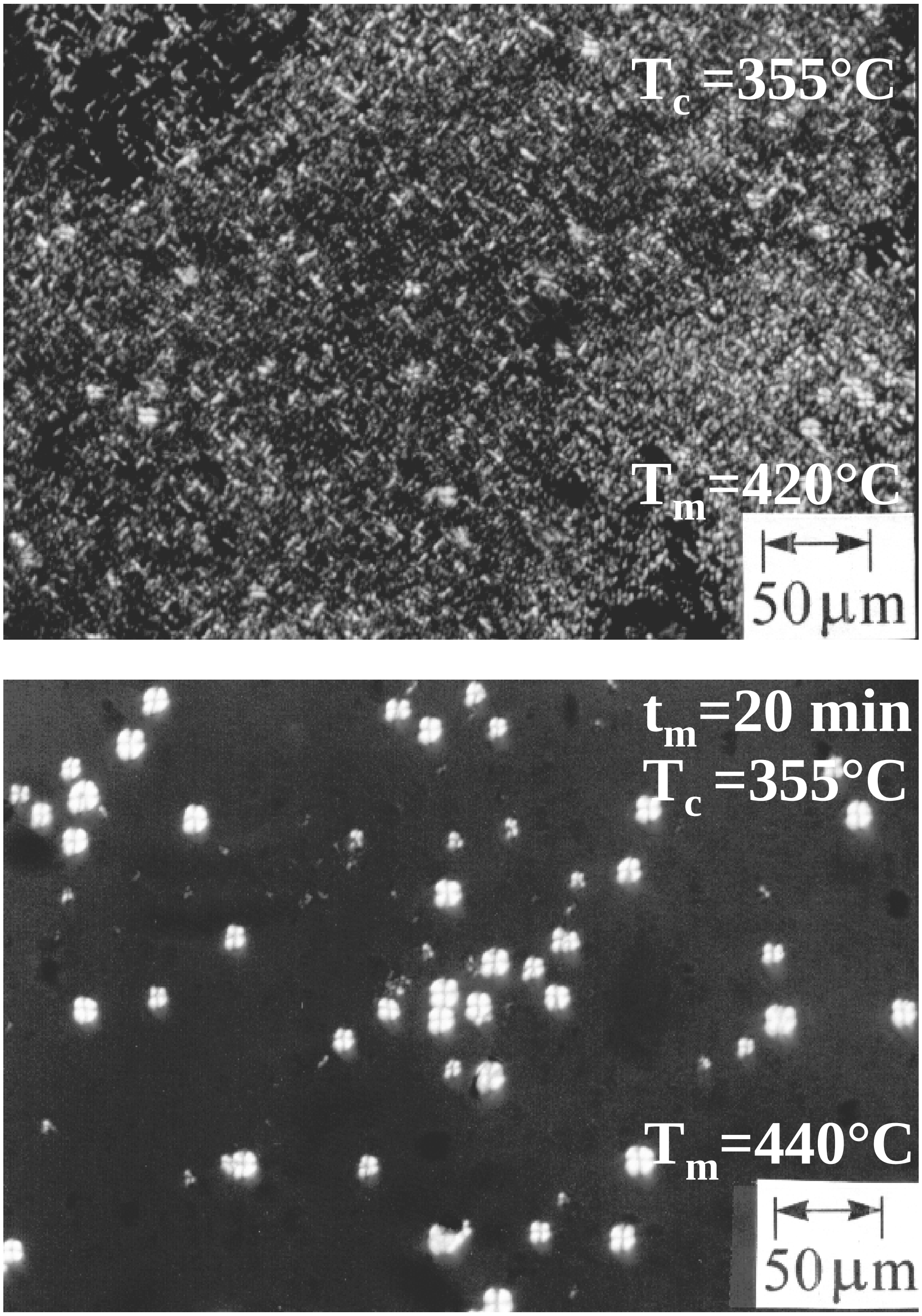

Figure 6.14 Polarized optical micrographs at 355°C after the indicated melt temperatures and a 20 minutes residence time.

410°C to 430°C, the initial crystallization response markedly slows. Interestingly, however, completion times for the overall crystallization do not show much change for the above range of melt temperatures. The corresponding Avrami plot (Figure 6.13) shows the effect of increased melt temperatures on the Avrami constants ‘K’ and ‘n’. The significantly increased value of ‘K’ with decreasing melt temperature is clearly reflective of a much higher nucleation density for lower melt temperatures. This is in fact confirmed by microscopy studies. Figure 6.14 shows the optical micrographs after 20 minutes at the melt temperatures of 420°C and 440°C. The change in nucleation density with a 20°C increase in melt temperature is strongly evident. The higher nucleation density thus contributes significantly towards the values of the bulk crystallization rate ‘K’. The decrease in the growth rates with increasing melt temperatures would also affect the bulk crystallization rates. This feature will be discussed later in the paper. It is clear however, that for isothermal crystallization experiments, melt temperatures have a tremendous effect on the subsequent morphology with regards to the final spherulitic size obtained. Also, an increase in nucleation density leads to the development of more sheaf-like structures and thus a lower Avrami exponent.

Although most flexible chain polymers provide a sufficient temperature range above the melting point where such effects due to residual nuclei or self-seeding nucleation are greatly suppressed, similar results have been obtained for other high melting polymers like PEEK[13, 14,22]. Although higher melt residence times and higher melt temperatures may be utilized to decrease the effect of previous thermal history, such conditions may also result in chemical reactions taking place. The ensuing discussion addresses this phenomenon.

6.3.2 Rheological studies

6.3.2.1 Isothermal frequency sweeps at 430°C

Semi-rigid chain polyimides like the one utilized in this study do not lend themselves to dissolution in any solvent and thus GPC analysis to quantify initial molecular weight or changes after various melt treatments is not possible. However, melt viscosity determination at various times and temperature serves as a good qualitative tool to detect changes in the molecular weight due to chemical changes at the desired melt temperature. Also, any changes in viscosity are important from a melt-processing viewpoint. Figure 6.15 shows the isothermal complex viscosity of TPER-BPDA-PA (15K) at 430°C as a function of frequency. The melt viscosity displays typical non-Newtonian behavior with the viscosity decreasing with increasing shear rates. At lower shear rates, the viscosity appears to be equilibrating towards a constant value (zero shear viscosity). The experiments were not performed at frequencies lower than 0.1 rad/s as the amount of time needed for these measurements is large and thus the polymer could undergo substantial changes in rheological response during the test at a given frequency. Also, in Figure 6.15, owing to the times needed for data collection at various frequencies, the complex viscosity ($|\eta^*|$) at 0.1Hz represents the values obtained after 8, 16, 24 and 32 minutes. It is very clear that the polymer is undergoing molecular weight changes at 430°C with the viscosity at the lower frequencies increasing by an order of magnitude within the time frame of the experiment. It is well known that η_0 often scales with $M_w^{3.4}$ for many linear thermoplastic polymers above the entanglement molecular weight. Thus assuming the initial M_w of ca. 30,000 daltons (as determined by GPC analysis of the poly (amic acid)) to be above the entanglement M_w, this enables correlating the initial zero shear rate viscosity with M_w (once it is also assumed that the polyimide chains are largely linear).

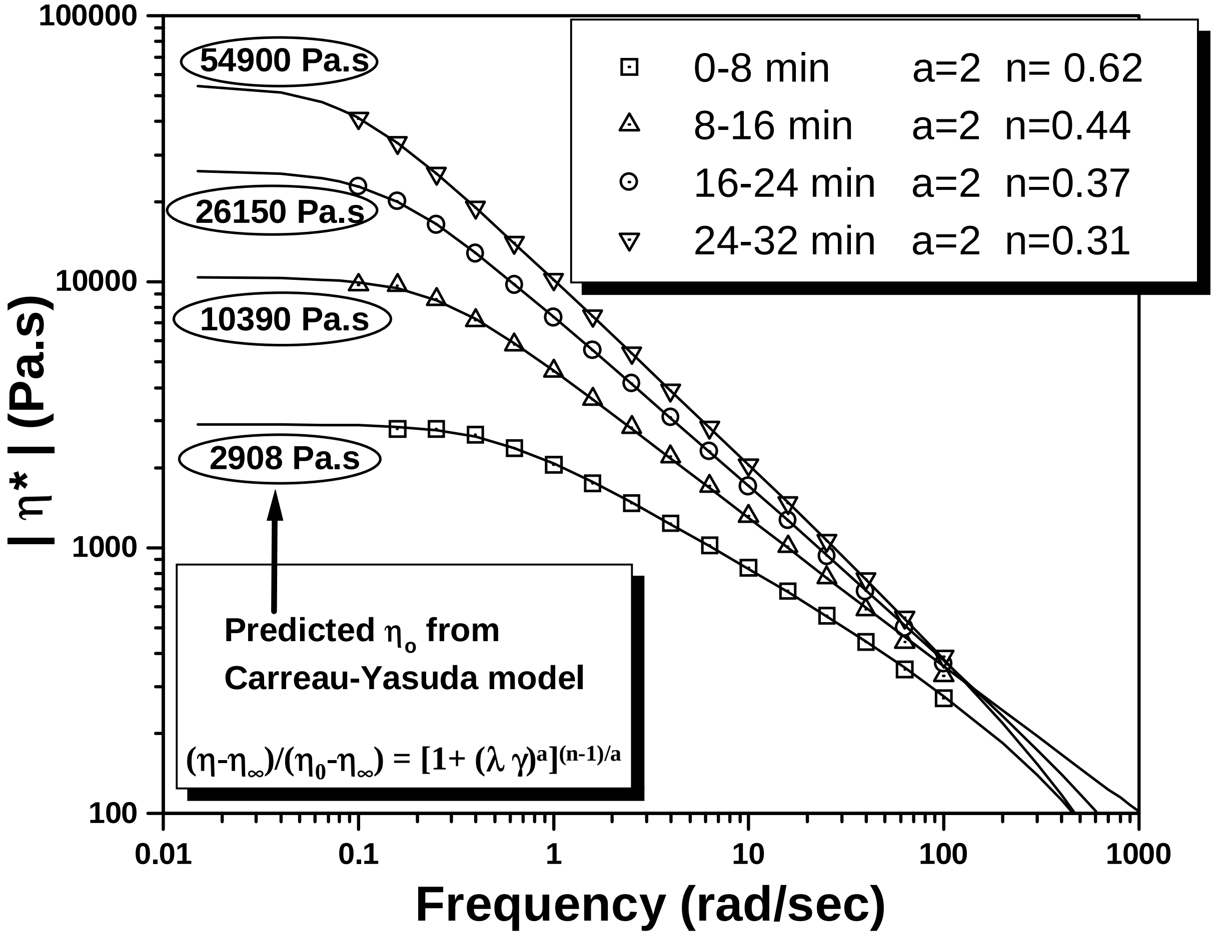

Figure 6.15 Non-Newtonian viscosity-frequency profile of TPER-BPDA-PA (initial M_n=15,000 daltons, M_w=30,000 daltons) at 430°C. The plot also indicates the data collection times for consecutive scans at the same temperature.

In order to obtain a ‘qualitative’ evaluation of molecular weight changes occurring in the material with time at 430°C, calculation of η_0 is thus required for the different curves. To estimate these variations in η_0, the Carreau-Yasuda model was utilized to fit the experimental data. This five parameter empirical model has proven very useful in the case of numerous polymer melts for providing analytical expressions for the non-Newtonian viscosity behavior. It has also been widely utilized to extrapolate the value of η_0 from available data that otherwise is often limited to experimentally attainable window of deformation rates. The model is given by the equation:

$$(\eta-\eta_\infty)/(\eta_0-\eta_\infty) = [1+ (\lambda\ \gamma)^a]^{(n-1)/a} \qquad \{6.5\}$$

Here λ is a characteristic “time constant”, ‘n’ is the power-law exponent and ‘a’ is a dimension less parameter that describes the transition breadth from the zero shear rate region to the power law region[30]. ‘η_0’ and ‘η_∞’ represent the zero-shear rate and infinite-shear rate viscosity respectively. Also for higher shear rates (100 rad/s); $\eta_\infty \ll \eta_0$ and thus η_∞ can be set equal to zero without introducing any significant error, though resulting in a simpler equation for fitting the data. While various values of ‘a’ were tried, good fits of the data were obtained for a=2. The calculated values of η_0 are indicated in Figure 6.15. While the estimated value of η_0 is ca.2900 Pa.s. after 8 minutes, it increases to ca. 55,000 Pa.s. after 32 minutes in the melt at 430°C! In this regard, if the $\eta_0 \propto M_w^{3.4}$ relationship is assumed and Carreau-Yasuda model is utilized to approximate η_0, a coarse estimate of the molecular weight changes occurring in the material can be obtained. *This rough analysis leads to the conclusion, that the initial weight average molecular weight (M_w) of ca. 30K, reaches ca. 44K after 16 minutes, ca.57K after 24 minutes and ca. 71K after 32 minutes!* These crudely estimated values indicate a more than two-fold increase in M_w after 32 minutes at 430°C. It is thus evident that relatively longer residence times of ca. 32 min at 430°C lead to significant occurrence of chemical reactions resulting in build up of molecular weight or crosslinking/branching reactions.

6.3.2.2 Isothermal time sweeps at various melt temperatures

Figure 6.16 shows the magnitude of the isothermal complex viscosity $|\eta^*|$ at temperatures ranging from 410°C to 450°C while keeping the frequency fixed at 1 rad/s. It is observed that the initial viscosity of the material is very sensitive to melt temperature. While the initial viscosity is ca. 2500 Pa.s at 410°C, it decreases to ca. 650 Pa.s when measured at 450°C. Although, higher temperatures would be expected to lead to a lower viscosity, destruction of residual nuclei at higher temperatures, leading to a more homogenous melt, could also contribute in lowering the viscosity. Earlier, optical microscopy experiments have shown that while the number of residual nuclei decrease with increasing melt temperatures and residence times in the melt, a large number of these nuclei do survive short exposure times at melt temperatures as high as 430°C. However, even short residence times at higher temperatures of 440°C and 450°C reduce the population of residual nuclei by a large amount. The effect of residual nuclei on melt viscosity is believed to be prominent at a melt temperature of 410°C. Although, earlier studies have indicated that the equilibrium melting point of this polymer is close to this temperature, the exact value of this temperature is not known with certainty. In this regard, if 410°C is below the true equilibrium melting point, a larger number of initial crystals may survive and could also contribute to a higher melt viscosity. This may lead to crystallization at lower supercoolings due to self-seeding nucleation. While the decreasing number of residual nuclei with time at any melt temperature would lead to a decrease in viscosity, molecular weight increases due to cross-linking reactions lead to an increasing viscosity with time in the melt.

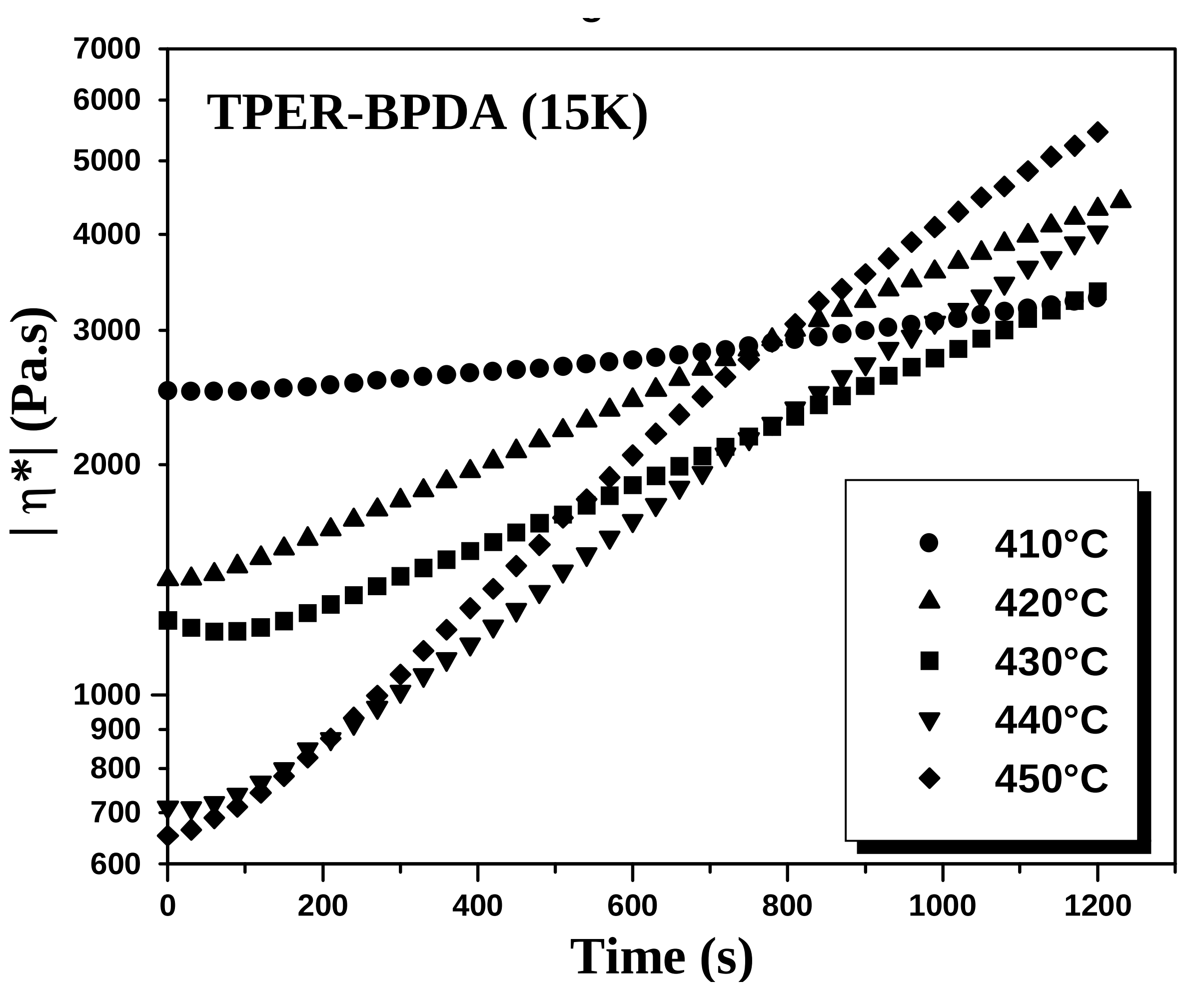

Figure 6.16 Isothermal complex viscosity (1 radian/s) as a function of residence time in the melt at various melt temperatures.

There is some indication that these chemical reactions are of some significance even at 410°C, after 15 minutes. At melt temperatures of 420°C and 430°C, the initial viscosity is much lower which is conjectured to be due to the destruction of residual nuclei (a more homogenous melt) and increased temperatures. However, it is clear that chemical (degradation) reactions (leading to molecular weight increase due to branching/crosslinking) begin at temperatures of 420°C and 430°C since the viscosity begins to rise soon after the melting of the polymer. The difference in severity of these reactions at 420°C and 430°C, however, is not great, as can be seen by the nearly parallel slope of viscosity vs. time curves for the two temperatures. The small difference in viscosity curves at these temperatures may be attributed to both the differences in temperatures and in the difference in the population of residual nuclei. At 430°C, the viscosity (at 1 rad/s) increases from ca. 1200 Pa.s to above 3000 Pa.s within 20 minutes, which, as shown earlier, is indicative of branching/crosslinking (degradation). Interestingly, however, earlier DSC studies[3, 4] from this laboratory has shown that the melting behavior after similar melt treatment remains unaffected, with no changes in the peak melting point, heat of melting or broadness of the melting endotherm! Hence it is clear that although these changes in the magnitude of complex viscosity indicate some chemical changes, the overall crystallizability and melting behavior of the polymer show little change. Increasing the temperature to 440°C or 450°C leads to a further initial drop in the melt viscosity due to the reasons discussed above. However, there is not much difference in the viscosity at 440°C and 450°C although there is a significant drop in the viscosity on increasing the melt temperature from 430°C to 440°C. This large decrease in initial viscosity is believed in large part due to a decrease in the population of residual nuclei. This would also lead to lower nucleation density on crystallization, this helping to confirm the earlier optical microscopy data in Figure 6.14.

The degradation reactions at 440°C and 450°C are significantly greater and lead to a faster increase in viscosity than at 420°C and 430°C. Interestingly, for melt temperatures of 420°C and 440°C, the final viscosity after a period of 20 minutes is nearly the same although the condition or structure of the melt is very different! While there is significantly less chemical reactions at 420°C, lower temperature and existing order in the melt is responsible for a higher viscosity. For a melt temperature of 440°C, however, the melt has an increased molecular weight due to crosslinking/ chain branching while most of the residual order is completely destroyed. The slope of complex viscosity vs. time can be approximately taken as the measure of the rate of degradation reactions at various temperatures. It is clear that the rate of chemical changes, although very similar at 420°C and 430°C, is largely increased when the melt temperature is increased to 440°C and 450°C. In fact the viscosity increases by nearly an order of magnitude in 20 minutes at 450°C. Also, although the time frame of 20 minutes was selected on the basis of earlier work, it is noticed that the state of the melt would be very different for shorter holding times. While holding times shorter than 3 minutes induce relatively little branching/crosslinking even at 450°C, successively higher melt temperatures also lead to a decreased viscosity. This lower viscosity would affect the melt processing as well as the final crystallization behavior on cooling.

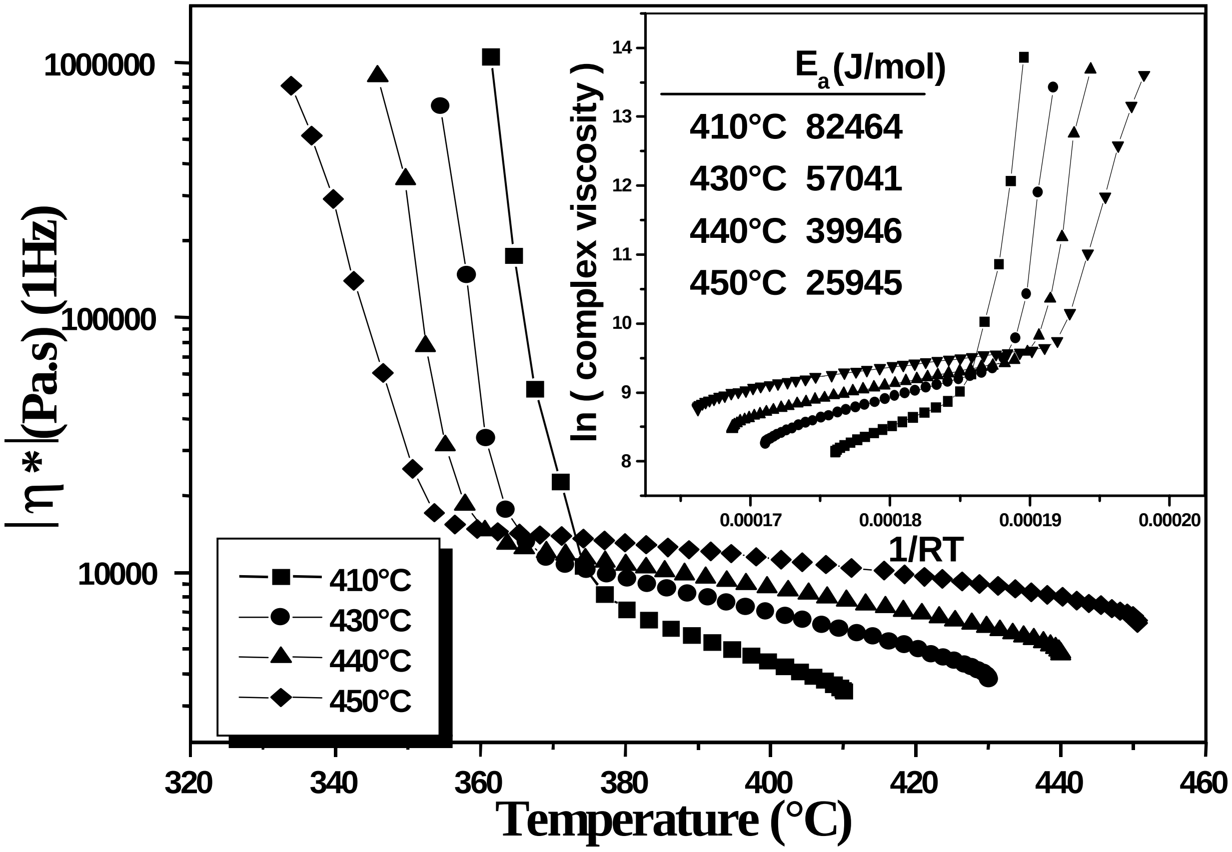

Figure 6.17 Non-isothermal complex viscosity (1 radians/s) when cooled at 10°C/min from various melt temperatures after 20 minutes residence time. *Inset*: Corresponding Arrhenius plots for the non-isothermal viscosity profiles when cooled from various melt temperatures. The initial regions prior to crystallization were utilized for estimating the value of activation energy using the Andrade-Eyring equation.

6.3.2.3 Complex viscosity on cooling from various melt temperatures

For processing operations it is important to know the variation of melt viscosity with cooling and also the temperatures at which solidification of the melt due to the crystallization may occur. The effect of thermal history on solidification temperatures is thus examined when the polymer melt was cooled at 10°C/min after 20 minutes at various melt temperatures and the results shown in Figure 6.17. The onset of crystallization was observed for all samples with the viscosity increasing sharply at various degrees of supercoolings. *A strong dependence, however, of the prior melt temperature on the crystallization is observed with the degree of supercooling necessary for crystallization increasing with higher melt temperatures.* Lower melt temperatures hasten the onset of crystallization with the onset temperature shifting from 377°C to 356°C when the melt temperature was changed from 410°C to 450°C. Crystallization at such low supercooling, when cooling from 410°C, clearly shows the strong effect of residual nuclei on crystallization behavior. Also, the supercooling required for crystallization was ca. 7-8°C more for a sample cooled from 450°C in comparison to a sample cooled from 440°C. This difference cannot be explained due to residual nuclei, as there is expected to be little difference in their population at these two temperatures (i.e. most of the residual nuclei are expected to be destroyed once the temperature is raised to 440°C, and thus no substantial decrement in their population is further expected by raising the temperature to 450°C). However, the higher molecular weight of samples caused by higher melt temperature leads to slower crystallization. Both the decreasing population of residual nuclei with increasing melt temperatures as well as the increased molecular weight of samples exposed to higher melt temperatures contribute to the onset temperature of crystallization. However, it should be clear that there is a strong frequency dependence in the above analysis and thus only qualitative trends can be made. For the same reason these results cannot be quantitatively compared with traditional DSC experiments, which are less sensitive in detecting the onset of crystallization.

6.3.2.4 Activation energy (E_a) values on cooling from various melt temperatures

It was also noted that the viscosity profiles before the onset of crystallization were also dependent upon the previous thermal history. It is well established that, the viscosity dependence on temperature can generally be described by the Andrade-Eyring equation[31]:

$$\eta = B \exp (E_a/RT) \tag{6.6}$$

This equation was derived initially for small molecules and is generally valid at temperatures in excess of 100 K above T_g for polymers. Here E_a is the flow activation energy of viscous flow and is representative of the energy barrier for successive segmental jumps into unoccupied sites or 'holes'. The value of E_a thus depends on the ease with which the polymer segments can "jump" into the available holes through conformational changes[32]. The higher value of E_a is indicative of a lower "jump frequency" and/or decreased availability of these holes. The lower "jump frequency" (higher E_a) can also be viewed as the result of a higher degree of co-operativity needed to create the required 'holes'. The general range of value of E_a varies between 20 KJ/mol to well over 120 KJ/mol for various polymers. The inset in Figure 6.17 also shows the corresponding Arrhenius plots based on this relationship. The regions of the curve before the onset of crystallization were used to *estimate* the activation energy for different curves. While the temperature range utilized to fit the data to the Andrade-Eyring equation was largest for crystallization from 450°C, sufficient data points were still available for a reasonable fit when following crystallization from 410°C. The activation energy was found to depend strongly on the initial thermal history. While the value of activation energy obtained was 82 KJ/mol when cooled from 410°C, it was only 26 KJ/mol when cooled from a melt temperature of 450°C!

It is well recognized that 'local segmental character' and not the molecular weight determines the value of activation energy. The value of activation energy, although dependent upon the chemistry, can also differ with changes in chain topology. Long chain branched polymer would be expected to show a higher value of activation energy than its linear homologue, the difference being dependent upon the amount and nature of the branching[33]. In this regard, the increase in molecular weight for a higher melt temperature would not explain to the lower values of activation energy obtained. However, the branching reactions that occur at these higher temperatures, would only serve to increase the translational/rotational restrictions along the chain backbone and thus should lead to a higher value of activation energy. However, an opposite trend is observed here! This result can be explained on the basis of residual order (residual nuclei) that still exists at lower melt temperatures. Increasing melt temperatures lead to destruction of this previous order and a more homogenous melt. The destruction of this residual order has already been confirmed on the basis of the earlier discussed optical microscopy results. The large differences observed in the value of activation energy are thus believed to be indicative of a more homogenous melt at higher temperatures. However, this homogeneity is accompanied with increased viscosity at these higher temperatures and is thus associated with increases in molecular weight.

It should be mentioned that evaluation of E_a would show some frequency dependence of such an analysis if carried out in the shear-thinning region. In this case however, results are based on viscosity at 1 rad/s, the lowest frequency experimentally feasible for such a study. *The values of* E_a *thus obtained serve more as a comparison between various experimental conditions rather than suggesting some truly absolute value for the polymer.*

6.3.3 Growth rates as a function of melt histories and non-isothermal behavior:

It was earlier demonstrated that harsher melt conditions lead to slower crystallization kinetics, which is in part due to the reduction in residual nuclei. Another important reason for slower crystallization response may be the decreased spherulitic growth rates due to increased melt viscosity caused by enhanced molecular weight/branching reactions following harsher melt conditions. To evaluate this effect, thin polymer films sandwiched between two glass slides were quenched to 345°C after 20 min residence times at 420°C-460°C. These melt conditions are similar to the experiments discussed earlier and adhesion experiments described elsewhere[4]. A spherulitic morphology was observed for all melt temperatures with no microscopically observable changes in the morphological character of the spherulites. *Interestingly, a spherulitic morphology was observed even after 20 minutes in the melt at 460°C!* This perhaps is the highest melt temperature from which organic polymer spherulites have been observed on cooling after such a long residence time in the melt. However, melt temperature and melt residence time have a strong effect on the subsequent spherulitic growth rate (Figure 6.18). The degradation (branching) associated with higher melt temperature/longer residence times results in significantly reduced growth rates. The growth rate studies also show a close correlation with earlier rheological results. For a residence time of 20 min, the growth rates show a sharp decrease if the melt temperatures are raised above 430°C. However, there is relatively a smaller drop in growth rate if the temperature is raised from 420°C to 430°C. This indicates that the extent of branching/cross-linking reactions, though somewhat similar at 420°C and 430°C, is largely increased if the melt temperatures are taken above 430°C. A similar conclusion was also reached after the previous rheological study and in earlier studies[3, 4.] Growth rate data was also collected after a 5 minute residence at 420°C and 430°C although the high nucleation density encountered due to these less stringment melt conditions necessitated several repetitions of this experiment. The growth rate after 5 min and 20 min residence times at 420°C were found to be 0.21μm/s and 0.107 μm/s respectively. Similar results are obtained for a melt temperature of 430°C. The significant reduction in growth rate with increased residence times is also in agreement with previous rheological results which indicate a corresponding two-fold increase in melt viscosity. Thus both techniques indicate the presence

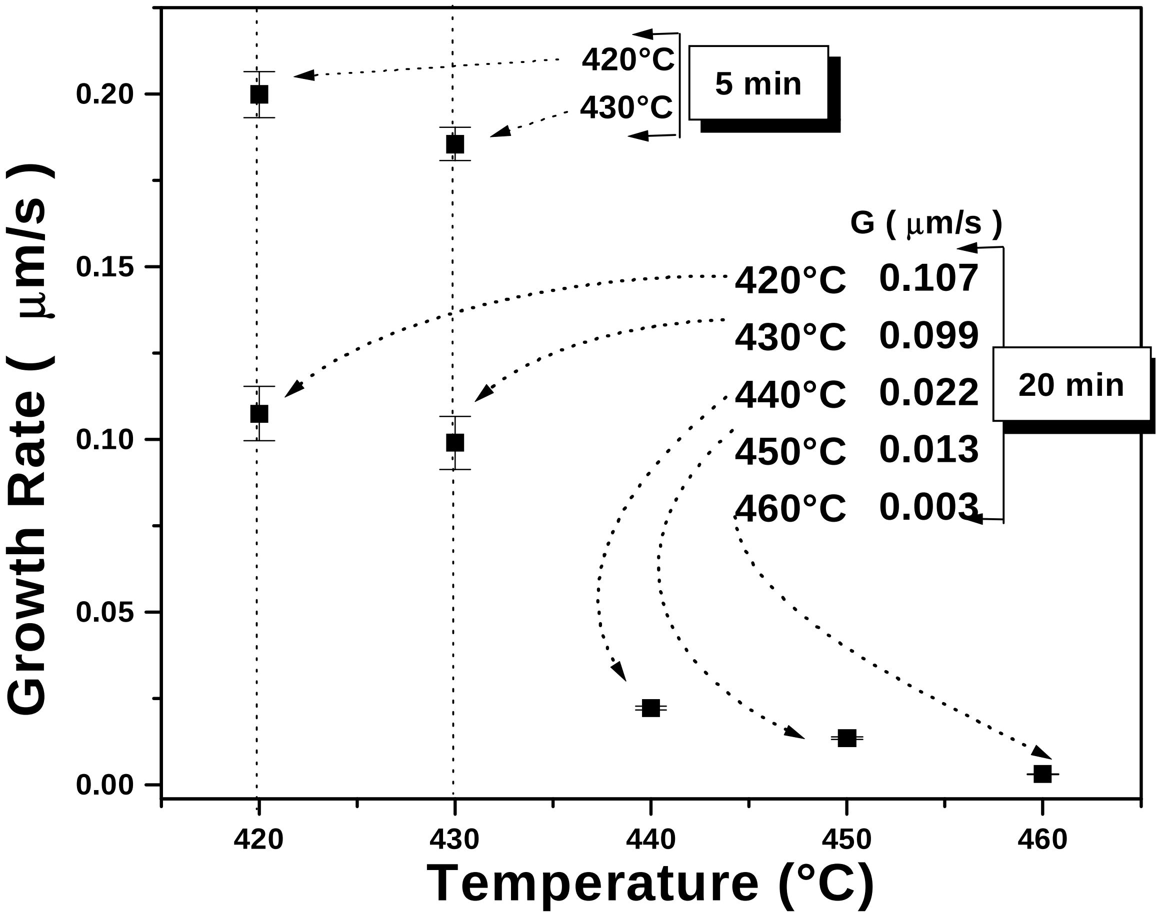

Figure 6.18 Spherulitic growth rates at 345°C after 20 minutes at various initial melt temperatures.

of some chemical reactions even at 420°C which is only 25°C above the bulk melting point of the polymer. These conclusions also highlight the importance of melt conditions for studies dealing with other high melting polymers. Proper selection of initial melt conditions is vitally important before any fundamental studies are attempted to model the crystallization behavior. However, for many such polymers including the one utilized in this study, such ideal conditions may not exist.

While the above spherulitic growth rate study helps in gauging the degradation effect of melt conditions, it also has important ramifications with regards to more conventional non-isothermal crystallization behavior. These results indicate that for a given cooling rate, as the initial melt temperature is increased, the crystallization would occur at larger supercooling. In fact, for harsher melt conditions, for e.g. 460°C for 20 min, the growth rates are significantly reduced and thus it should be possible to quench the polymer to a state with little or no crystallinity present. However, a significant amount of crystallinity was found to be present by DSC and a very fine grainy morphology was revealed by optical microscopy for such a quenched sample. Non-isothermal studies were thus attempted to interpret this behavior.

DSC was utilized to observe the non-isothermal crystallization behavior from different initial melt temperatures. Figure 6.19 shows the cooling scans at 10°C/min after 10 minutes in the melt at temperatures varying from 400°C to 450°C. As the temperature is increased beyond 400°C, the crystallization exotherm shifts to higher undercoolings, the amount of shift increasing with increasing melt temperatures. While the scans from 400°C and 450°C give a characteristic single crystallization peak, the intermediate scans lead to a double peak in the crystallization exotherm! A melt temperature of 400°C, which is above the bulk melting point of 395°C (but below the expected equilibrium melting point), does not erase the previous thermal history and thus the crystallization occurs at much smaller undercoolings. The sharper (and higher) crystallization exotherm (from 400°C) is believed to result from the recrystallization of previously unmelted residual crystals. However it is interesting to note that a second crystallization peak appears for intermediate melt

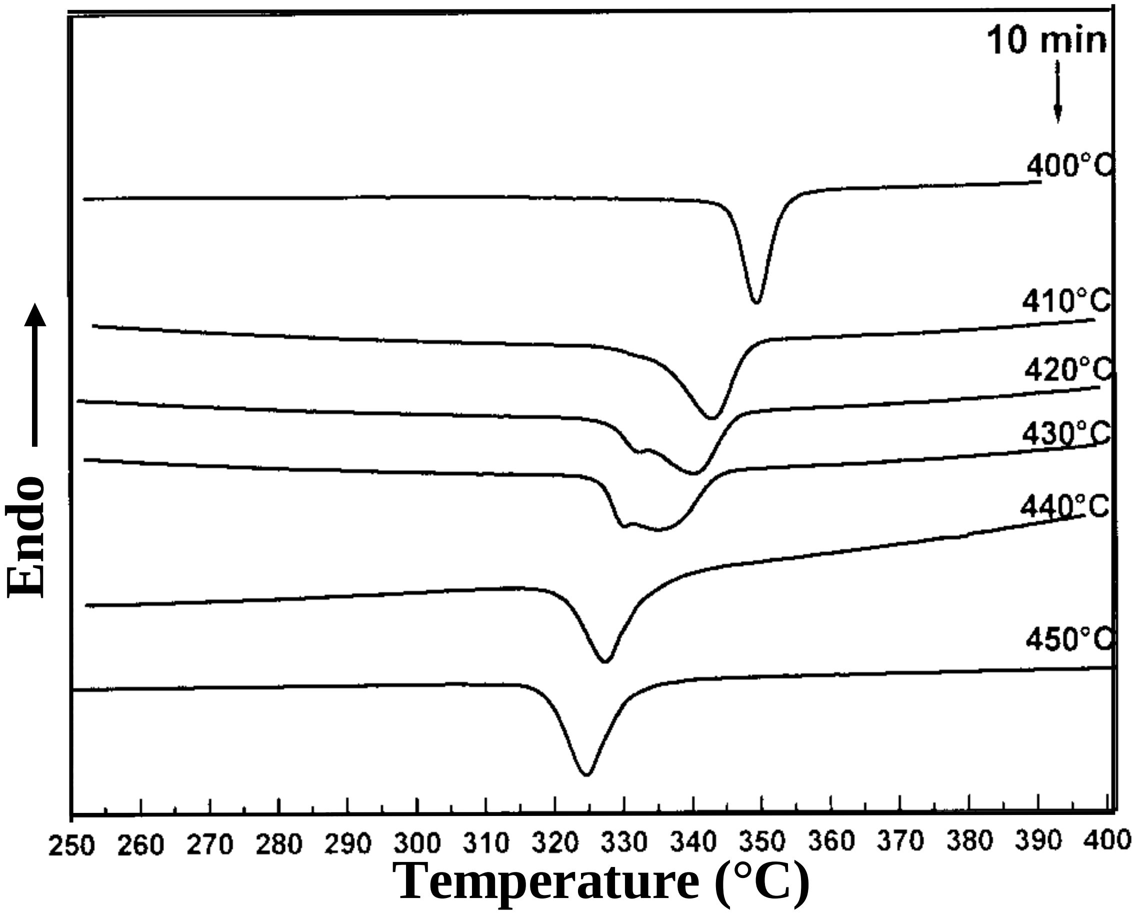

Figure 6.19 DSC cooling scans at 10°C/min after 10 minutes at various melt temperatures.

temperatures. This second peak appears first as a shoulder on the low temperature side of the exotherm when cooling from 410°C, but becomes a separate peak as the melt temperature is increased. It is clear that the double exothermic behavior is indicative of two separate crystallization phenomenon. The occurrence of these crystallization exotherms, however, is dependent on previous melt history. Also, earlier studies[4,5] have not indicated any evidence of polymorphism in this polymer.

Isothermal crystallization experiments were performed at temperatures in the vicinity of the double exothermic behavior (at 335°C) using a hot-stage on an optical microscope between crossed polars. It was found that the initial spherulitic crystallization was followed by a sudden 'catastrophic nucleation' leading to the development of a fine grainy background! The details of the superstructure that developed due to this catastrophic nucleation were not optically resolvable and caused the initially observable larger spherulites to become totally enveloped in the subsequent overall fine pattern. The double exothermic behavior on non-isothermal crystallization from the melt is easily explained due to this catastrophic nucleation process. When cooling from 420°C, the initial exotherm is indicative of spherulitic development, while the onset of 'catastrophic nucleation' at lower temperatures leads to a second exothermic peak. As shown earlier, increasing the melt temperature to 440°C and 450°C leads to a significant reduction in the nucleation density (Figure 6.14) and much decreased spherulitic growth rates (Figure 6.18). *Thus, a lesser number of heterogeneous sites available for spherulitic development and reduced spherulitic growth rates decrease the chances of any spherulitic crystallization at lower supercooling (i.e. at* T_c*>340°C) during a non-isothermal cooling scan in a DSC.* This is distinctly observed in DSC cooling scans (Figure 6.19) as the melt temperatures are increased to 440°C and 450°C. While at temperatures lower than 430°C, initial spherulitic crystallization contributes significantly to the overall crystallization, the second 'catastrophic nucleation' process is mainly responsible for crystallization from 440°C and 450°C. The crystallization peak, however, shifts to 324°C from 327°C as the melt temperature is increased from 440°C to 450°C, thus indicating a small dependence of 'catastrophic nucleation' on the initial melt temperature.

To study the crystalline morphology when crystallization occurs under nonisothermal conditions, a typical experiment was performed from the melt at a cooling rate of 20°C/min. The melt conditions observed for this experiment were 430°C and 20 minutes respectively. While spherulitic development begins early, a subsequent decrease in the temperature in the vicinity of 330°C leads to a catastrophic increase in nucleation density as shown in the last micrograph of Figure 6.20. As observed in isothermal experiments, this rapid increase in nucleation density leads to development of a fine pattern, which envelops the initially growing spherulites. However when cooled from higher melt temperatures (eg. 450°C), at the same cooling rate, no spherulites were observed and only the 'catastrophic nucleation' was responsible for the crystallization. The initial melt conditions and cooling rate thus are critical in deciding the final morphology of this polymer.

6.4 Conclusions

Isothermal crystallization of semicrystalline polyimide, TPER-BPDA-PA was characterized as a function of crystallization temperature and thermal history in the melt. It was found that isothermal crystallization was very sensitive to crystallization temperature thereby limiting the thermal window of study. The holding time in the melt also had a strong affect on crystallization behavior. At a given supercooling, increased holding time in the melt at 430°C substantially broadened the crystallization exotherm. While the Avrami exponent did not show a significant change, the value of the Avrami parameter 'K' decreased considerably with residence time in the melt. Melt temperatures also affected the crystallization behavior substantially with the Avrami analysis showing strong changes in both the exponent 'n' and the parameter 'K'. A substantial decrease in the nucleation density with harsher melt conditions was revealed by optical microscopy and was primarily responsible for slowing the crystallization kinetics at 355°C.

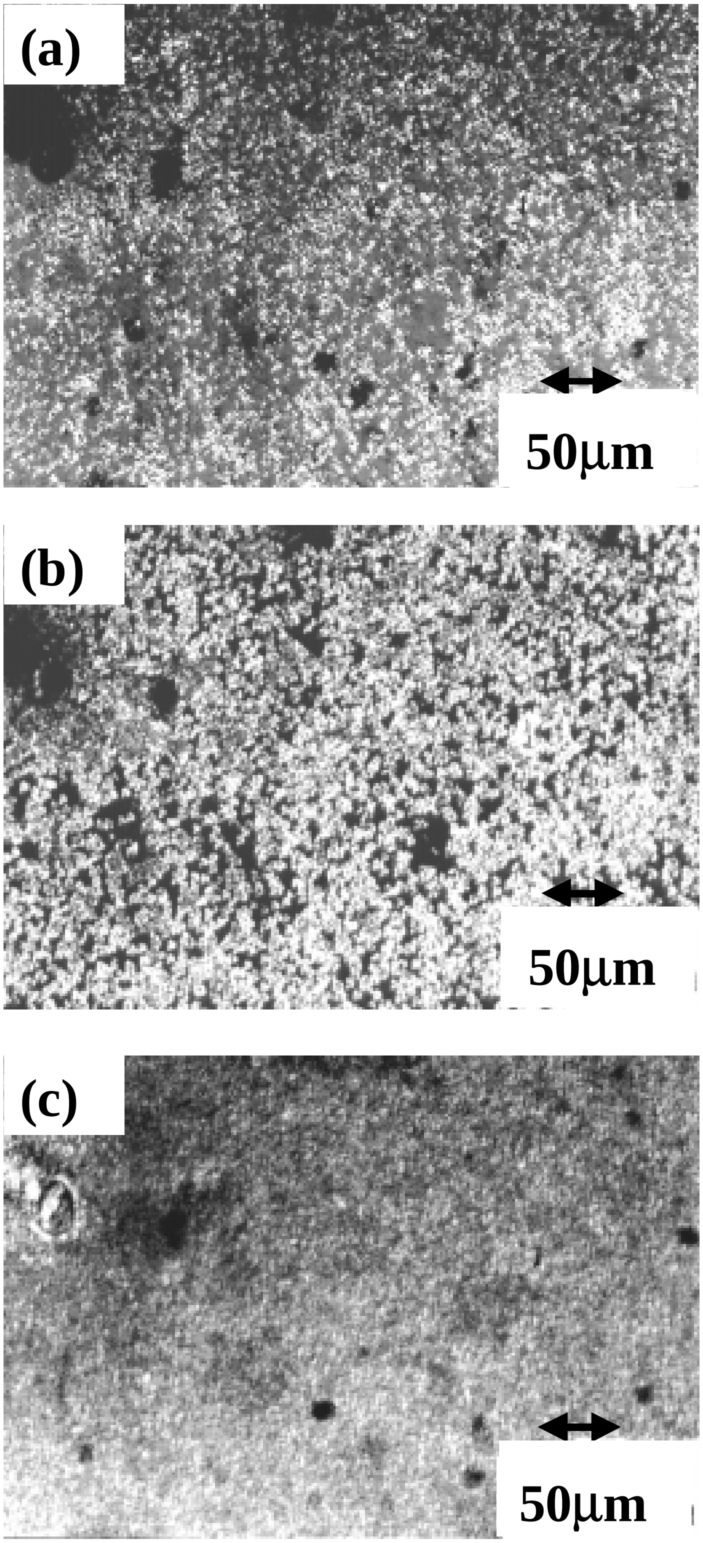

Figure 6.20 Polarized optical micrographs illustrating the morphological development when cooled at 20°C/min from the melt at 430°C for 20 minutes. Micrographs taken at (a) 340°C (b) 332°C (c) 323°C.

Melt viscosity experiments conducted at 430°C showed that chemical reactions (branching/cross-linking) were indeed present at these temperatures. The rate of these reactions however, increased substantially above 440°C. At lower melt temperatures of 410°C, however, little evidence of any major chemical changes was evidenced. However, although higher temperatures lead to build up of molecular weight, they also succeed in removing the previous thermal history to a large extent. Crystallization experiments performed using a rheometer showed that the onset of crystallization shifts to higher undercoolings with increasing melt temperatures. The temperature dependence of the complex viscosity as a function of previous melt temperature was evaluated using the Andrade-Eyring equation. The estimated activation energies found by such an analysis decreased strongly with increasing melt temperatures. This was due to the decreasing constraints of the residual nuclei, whose population decreased with increasing melt temperature.

Isothermal experiments at 345°C showed that growth rates were also dependent upon the previous melt temperature, with large decreases in growth rates observed when the initial melt temperature was raised above 430°C. The growth rates did not show any significant change when the initial melt temperature was changed from 420°C to 430°C. However, experiments carried out for shorter residence times at 420°C and 430°C showed higher growth rates due to lesser degradation. Interestingly, spherulites (with no observable change in the overall superstructure) were even obtained from melt temperatures as high as 460°C after residence times as long as 20 minutes.

Non-isothermal DSC experiments revealed double peaks in the crystallization exotherms. A ‘catastrophic nucleation’ process was found to explain the presence of the second peak as revealed by both isothermal and nonisothermal POM studies. This second crystallization process dominated the overall crystallization as the melt temperatures were raised. The crystalline morphology resulting from this ‘catastrophic nucleation’ process could not be resolved by optical microscopy.

6.5 Acknowledgments

The author wishes to thank the NSF Science and Technology Center for High Performance Polymeric Adhesives and Composites for full support of this study under contract number DMR 9120004. Generous support from the GenCorp Foundation is also acknowledged.

References:

---

[1] Hergenrother, P.M., Stenzenberger, H.D. and Wilson D., *Polyimides*, Blackie & Son Ltd., London, 1990.

[2] Mittal, K.L. and Ghosh, M.K., *Polyimides: Fundamentals and Applications*, Marcel Dekker, Inc., 1996.

[3] Wilkes, G.L. *Ency. Phy. Sci. Tech*. 1987, Vol. **11**, 61.

[4] Ratta, V., Stancik, E.J., Ayambem, A., Parvatareddy, H., McGrath, J.E. and Wilkes, G.L. *Submitted to Polymer.*

[5] Srinivas, S., Caputo, F.E., Graham, M., Gardner, S., Davis, R.M., McGrath, J.E. and Wilkes, G.L. *Macromolecules*, 1997, **30**, 1012.

[6] Sasuga, T. *Polymer*, 1991, **32**, 1539.

[7] Chang, A.C., Hou, T.H., St. Clair, T.L. in *Polyimides: Trends in Materials and Applications, Proc. Fifth Int. Conf. on Polyimides*, 1994, 3.

[8] Graham, M.J., Srinivas, S., Ayambem, A., Ratta, V., Wilkes, G.L. and McGrtah, J.E. *Polymer Preprints,* April, 1997, **38(1),** 306.

[9] Grenier, D. and Homme, R.E.P. *Journal of Polymer Science: Polymer Physics Edition,* 1980,**18**, 1655.

[10] Price, F.P. *Journal of Applied Physics* 1965, **36**, 3014.

[11] Tomka, J. *European Polymer Journal,* 1968, **4**, 237.

[12] Hillier, I.H. *Journal of Polymer Science: Part A,* 1965, **3**, 3067.

---

[13] Banks, W., Hay, J.N., Sharples, A., and Thompson, G. *Polymer*, 1964, **5**, 163.

[14] Risch, B.G., Warakomski, J.M. and Wilkes, G.L. *Polymer*, 1993, **34**, 2330.

[15] Hsiao, B.S., Kreuz, J.A., and Cheng, S.Z.D., *Macromolecules* 1996, **29**, 135.

[16] Muellerleile, J.T., Risch, B.G., Rodrigues, D.E., and Wilkes, G.L., *Polymer* 1993, **34**, 789.

[17] Lee, Y. and Porter, R.S. *Macromolecules* 1988, **21**, 2770.

[18] Cebe, P. and Hong, S. *Polymer* 1986, **27**, 1183.

[19] Heberer, D.P., Cheng, S.Z.D., Barley, J.S., Lien, S.H.S., Bryant, R.G. and Harris, F.W. *Macromolecules* **24**, 1890.

[20] Hsiao, B.S., Sauer, B.B. and Biswas, A. *Journal of Polymer Science: Part B: Polymer Physics*, 1994, **32**, 737.

[21] Lopez, L.C. and Wilkes, G.L. *Polymer* 1988, **29**, 106.

[22] Wunderlich, B. 'Macromolecular Physics: Crystal Nucleation, Growth and Annealing', Vol. 2, Academic Press, New York, 1976.

[23] Fatou, J.G. *"Crystallization Kinetics", Encyclopedia of Polymer Science and Engineering, (Suppl. Vol.)*, John Wiley and Sons, New York, 1989, 231.

[24] Hoffman, J.D., Davis, G.T. and Lauritzen, J.I., Jr., '*Treatise in Solid-State Chemistry*', (ed. Hannay, H.B.), Vol. 3, Plenum Press, New York, 1976, 497.

[25] Ergoz, E., Fatou, J.G. and Mandelkern, L. *Macromolecules* 1972, **5**, 147.

[26] Jonas, A. and Legras, R. *Polymer* 1991, **32**, 2691.

[27] Turnbull, D. *J. Chem. Phys.* 1950, **18**, 198.

[28] Morgan, L.B. *J. Appl. Chem.*, 1954, **4**, 160.

[29] Jorda, R., and Wilkes, G.L. *Polymer Bulletin* 1988, **19**, 409.

[30] Bird, R.B., Armstrong, R.C., Hassager, O. in *"Dynamics of Polymeric Liquids"* John Wiley and Sons, New York, Vol. 1, Fluid Mechanics, 1987, 171.

[31] Mendelson, R. *Polymer Engineering Science* 1968, **8**, 235.

[32] Cowie, J.M.G., *in "Polymers: Chemistry and Physics of Modern Materials"*, 2nd edition, Blackie A & P, 1997, 255.

[33] Wilkes, G.L. *Journal of Chemical Education* 1981, **58**, 880.